Revised MS No: VR-20-113 R1 January 2021

Contrast adaptation and interocular transfer in cortical cells: a re-analysis & a two-stage gain-control model of binocular combination

Mark A Georgeson[*] & Frank Sengpiel[§]

[*] College of Health & Life Sciences, Aston University, B4 7ET, UK
[§] School of Biosciences, Cardiff University, CF10 3AX, UK

Abstract

How do V1 cells respond to, adapt to, and combine signals from the two eyes? We tested a simple functional model that has monocular and binocular stages of divisive contrast gain control (CGC) that sit before, and after, binocular summation respectively. Interocular suppression (IOS) was another potential influence on contrast gain. Howarth, Vorobyov & Sengpiel (2009, *Cerebral Cortex*, *19*, 1835–1843) studied contrast adaptation and interocular transfer in cat V1 cells. In our re-analysis we found that ocular dominance (OD) and contrast adaptation at a fixed test contrast were well described by a re-scaling of the unadapted orientation tuning curve – a simple change in response gain. We compared six variants of the basic model, and one model fitted the gain data notably better than the others did. When the dominant eye was tested, adaptation reduced cell response gain more when that eye was adapted than when the other eye was adapted. But when the non-dominant eye was tested, adapting either eye gave about the same reduction in overall gain, and there was an interaction between OD and adapting eye that was well described by the best-fitting model. Two key features of this model are that signals driving IOS arise 'early', before attenuation due to OD, while suppressive CGC signals are 'late' and so affected by OD. We show that *late* CGC confers a functional advantage: it yields partial compensation for OD, which should reduce ocular imbalance at the input to binocular summation, and improve the cell's sensitivity to variation in stereo disparity.

Key words

Visual cortex; contrast adaptation; interocular transfer; ocular dominance; contrast gain control; binocular combination

Acknowledgments

This re-analysis was supported by a grant to MAG from the Leverhulme Trust, EM-2017-097. The original physiological work was supported by grants to FS from the Medical Research Council (UK), G0000100, G0500186; Human Frontier Science Program, RG 0070/1999-B.

1. Introduction

1.1 Neural basis of binocular vision & stereopsis

Physiological studies over the last 60 years have established that single neurons in the primary visual cortex (V1) of cats and monkeys combine sensory inputs from the left and right eyes to provide the functional basis for binocular fusion and binocular depth perception (Anzai, Ohzawa, & Freeman, 1999; Barlow, Blakemore, & Pettigrew, 1967; Hubel & Wiesel, 1962, 1968; Ohzawa, DeAngelis, & Freeman, 1990, 1996; Pettigrew, Nikara, & Bishop, 1968; Poggio & Poggio, 1984). Many of these neurons are disparity-selective: their responses vary systematically with the degree of displacement (*binocular disparity*) between the spatial positions or spatial phases of the pair of input images (Anzai, Ohzawa, & Freeman, 1997, 1999a; Prince, Cumming, & Parker, 2002). A population of such cells with different disparity preferences encodes information about relative depth in 3-D scenes. For reviews of binocular cell responses in relation to stereopsis and models of stereopsis, see Marr & Poggio, 1979; Ohzawa, 1998; Poggio & Poggio, 1984; Read & Cumming, 2003; Roe, Parker, Born, & DeAngelis, 2007.

Thirty-five years ago, Ohzawa and Freeman argued that to understand the neural basis of binocular vision and stereopsis we first need good models of the signal processing that leads to binocular combination of signals from the two eyes (Freeman & Ohzawa, 1990; Ohzawa & Freeman, 1986). We adopt the same view here, and we explore the functional architecture laid out in Fig. 1, with the following themes.

1.2 Output nonlinearity

Freeman & Robson (1982) pioneered the study of binocular cortical cells in response to drifting sinewave gratings as a function of interocular phase difference (phase disparity). Using this approach, Ohzawa & Freeman (1986) found that a linear model, comprising linear spatial filtering by monocular receptive fields for each eye, followed by linear summation across the eyes, accounted well for the responses of binocular simple cells, but only if a threshold nonlinearity was applied to the signal after binocular summation (Ohzawa & Freeman, 1986; Smith, Chino, Ni, & Cheng, 1997). Later studies of orientation and direction selectivity of cortical cells led to some consensus that the form of this nonlinearity was a smooth expansive function (such as a power function) rather than half-wave rectification (e.g. Anzai, Ohzawa, & Freeman, 1999; Gardner, Anzai, Ohzawa, & Freeman, 1999). Miller & Troyer (2002) resolved the issue by showing that if the membrane potential is noisy then, in the conversion to spike rate, thresholded half-wave rectification is effectively smoothed to a power function. Such a nonlinearity confers contrast-invariant tuning, and sharpens the selectivity of the neuron for its preferred stimulus, and is a standard feature of functional models of V1 cell responses (Albrecht & Geisler, 1991; Heeger, 1992).

1.3 Monocular & Binocular gain controls

V1 cell responses to gratings are often strongly selective for interocular phase disparity, showing a peak response at a particular disparity ϕ, and a minimum response at a phase disparity of $\phi \pm 180$ deg. This is expected from a linear system that sums signals from each eye. Surprisingly, however, substantial modulation by disparity has been observed in cat & monkey cortical cells even when the contrasts are grossly mis-matched between the eyes (Ohzawa & Freeman 1986; Freeman Ohzawa 1990; Smith et al, 1997a,1997b). For the cells analysed in detail by Truchard *et al* (2000), responses were strongly modulated by disparity even when the contrast in one eye was as much as 10 or 20 times lower than in the other eye. This is indeed surprising, because the result of summing a weak sinusoidal signal with a strong one is dominated by the strong signal. The phase of the weak signal can only weakly modulate the summed response. However, monocular

contrast gain control changes all that. Increasing contrast is counteracted by gain reduction. Increasing contrast for one eye drives down the gain for that eye, and so the response amplitude increases rather little. Hence response amplitudes for weak and strong signals in the two eyes are more similar than the difference in their contrasts would suggest. This similarity allows the 'weak' input to modulate the binocular sum more effectively than in a linear system. Using this principle, Truchard *et al* (2000) calculated the monocular and binocular gain values (*M*, *B* in Fig. 1) that would be needed to account for their results on a sample of cat simple cells. They found that monocular gain greatly decreased as contrast increased, while binocular gain was little affected by contrast. They concluded that contrast gain control operates mainly in the monocular pathways leading to binocular combination.

1.4 Ocular dominance

Binocular V1 cells are often driven more strongly by one eye than the other (*ocular dominance, OD*). Surprisingly perhaps, even cells that respond exclusively to one eye when tested monocularly often exhibit strong binocular interactions and disparity sensitivity when both eyes are tested together (Ohzawa & Freeman, 1986; Smith, Chino, Ni, Ridder, & Crawford, 1997). This implies that there is a weaker but still functional input from the non-dominant eye (NE) that is 'hidden' by a response threshold or threshold-like output nonlinearity, as above. In binocular testing this input can modulate the response to the other eye, even though the NE stimulus alone may drive the spike response only weakly or not at all. With monocular testing, the output nonlinearity thus exaggerates the apparent mismatch in strength of left and right eye connections to the binocular cell (Priebe, 2008).

1.5 Contrast adaptation

Exposure to the contrast of a grating reduces behavioural contrast sensitivity, and does so selectively when the adapting and test gratings are similar in orientation and spatial frequency (Blakemore & Campbell, 1969; Georgeson & Harris, 1984). In psychophysics, contrast adaptation is often taken to involve a slow build-up and slow recovery of the adaptation effect, but the dynamics are likely to be more complex than that, since even brief exposures (e.g. 1 sec) can produce brief but substantial sensitivity loss, and the time taken to recover from adaptation depends much more on the time spent adapting than it does on the contrast of the adapter (Greenlee, Georgeson, Magnussen, & Harris, 1991).

Adaptation and contrast gain control are closely linked. In psychophysics, the increase of sensitivity loss with adapting contrast, and its dependence on relative spatial frequency, were strikingly similar after (i) adapting for two minutes, or (ii) 'adapting' for 25 msec provided the test was flashed within 50 msec (Georgeson & Georgeson, 1987). This points to some shared underlying mechanism in contrast adaptation and 'instantaneous' gain control.

At the V1 cell level, exposure to contrast causes both contrast gain and response gain to decrease (Albrecht, Farrar, & Hamilton, 1984; Bonds, 1991; Ohzawa, Sclar, & Freeman, 1985; Sclar, Lennie, & Depriest, 1989). More recent studies have revealed greater complexity of the suppression mechanisms involved over different spatial and temporal scales (Patterson, Wissig, & Kohn, 2013) and orientations (Westrick, Heeger, & Landy, 2016), but a divisive normalization (gain control) framework still seems appropriate (for review see Solomon & Kohn, 2014), perhaps especially for the simple adaptation protocol used in our target study (Howarth, Vorobyov, & Sengpiel, 2009).

1.6 Plan for this paper

We are interested in the binocular properties of V1 cells in response to luminance contrast, and in their adaptation to contrast, with the aim of formulating a relatively

simple, functional model that helps us to understand better the basis for binocular processing and combination of signals at the cortical cell level. To do this we:
(i) re-analyzed data from Howarth, Vorobyov, & Sengpiel (2009), which appears to be the only published quantitative study to date of contrast adaptation and its interocular transfer in V1 cells;
(ii) formulated a general binocular cell model (Fig. 1) along with several specific versions of it (Fig. 2) whose components are: monocular and binocular levels of gain control, ocular dominance, interocular suppression, binocular summation, and an expansive output nonlinearity;
(iii) fitted these models to the data of Howarth et al (2009), constrained in part by other relevant V1 results; and
(iv) compared the six model variants (Fig. 2) to infer the best-supported model, and so obtain a clearer view of how the gain control works, how it interacts with OD, and whether interocular suppression plays a role in contrast adaptation at the single-cell level.

2. Methods

2.1 Data

A dataset of micro-electrode responses recorded extracellularly from 54 cells in the cat primary visual cortex was available from the study of Howarth, Vorobyov, & Sengpiel (2009). Recordings were made from neurons throughout the depth of V1 (area 17), in the region representing the central visual field. To sample a wide range of ocular dominances the cortical penetrations targeted left- and right-eye columns as well as binocular zones, as determined by optical imaging of intrinsic signals. Each cell was tested with sinusoidal gratings of fixed contrast (typically 0.5 c/deg, contrast 0.5 or 1.0), filling a 20 by 20 deg display area, drifting at 2 Hz, at each of 8 orientation/directions (-180^0 to $+135^0$ in 45^0 deg steps). Cell response to a given test stimulus was defined as the mean firing rate (spikes/sec) during the 1.5s test periods minus the 'spontaneous rate' (mean rate during 1.5s blank, zero-contrast periods). These test responses were collected after a period of adaptation to a grating of optimal spatial frequency (contrast 0.25 or 0.5) drifting in the preferred orientation and direction for the cell, and after control periods where the adapting contrast was zero. The gratings were always monocular, and all 6 possible combinations (test L or R eye, adapt L or R or neither eye) were assessed. For further details, see Howarth et al., 2009.

For the present study, cells were classified according to their ocular dominance, defined by an ocular dominance index (ODI) of the responsiveness of the cell to monocular stimuli in the less sensitive eye, relative to the more sensitive one. Specifically, the ODI was the ratio of total response to drifting gratings (summed over the 8 stimulus directions) for the non-dominant eye (NE) divided by that for the dominant eye (DE), without prior adaptation to contrast. Thus:

$$ODI = \sum_{i=1}^{8} R_{NE}(\theta_i) / \sum_{i=1}^{8} R_{DE}(\theta_i).$$

With this definition ODI ranges from 0 (no response to NE) to 1 (same response to NE and DE). For our present analyses, cells were ordered by ODI value and then divided into *N* groups (*N*=3 to 10, or higher), ranging from groups whose *monocular* responses were mainly confined to one eye to those driven substantially by either eye.

*** Fig. 1 about here ***

2.2 Modelling: design and implementation

An outline of the model we applied to these data is shown in Figure 1. In brief, monocular gains (*M*) are reduced both by the current test contrast in a given eye and by the adapting grating (if any). Whether the current or prior contrast in one eye can reduce the *M* gain for the other eye depends on whether a route for interocular suppression (IOS) is present, or not. We assume that, after binocular summation, binocular gain (*B*) can be reduced by adapting through either eye, and we incorporate the important finding that, unlike *M*, binocular gain *B* is altered little or not at all by the current test stimulus (Truchard *et al*, 2000).

Many cortical cells respond more vigorously to one eye than the other. Such ocular dominance (OD) has been studied intensively and much is known about the anatomy and physiology of OD in V1, its organization into cortical OD columns, and the way their development in the young animal is influenced by normal or abnormal early visual experience. But in the model scheme of Fig. 1, we do not know *a priori* where the OD asymmetry should be placed nor how it might influence the setting of gains for each eye. To address these questions we developed several more specific model structures based on Fig. 1, in which the contrast-response from one eye (NE) is attenuated relative to the dominant eye (for example, $d_R < d_L$ in Fig. 1). In these candidate models, the monocular contrast gain control (CGC) is either driven 'early' by the unattenuated contrast (Fig. 2C), or 'late' by the contrast-response after its attenuation by OD (Fig. 2F). Three consequences of the OD attenuation, as we shall see, are (i) that the model cell responds less to stimulation through one eye (NE) than the other, (ii) that it adapts less (at stage *B*) on exposure to contrast in that eye than the other, and (iii) with early CGC the adaptation of the monocular NE gain stage *M* is the *same* as for the dominant eye, unaffected by the degree of dominance *d,* while for late CGC the adaptation at level *M* is less when OD is more unbalanced. The ocular dominance factors d_L, d_R and the orientation tuning *S* are assumed to be unaffected by prior adaptation, and we fixed test contrast at 1.0 and adapting contrast at 0.5.

*** Fig. 2 about here ***

After the adjustments of monocular response amplitude, signals from the two eyes are summed linearly (Ohzawa & Freeman, 1986). This binocular response is subject to the second gain adjustment *B* and then in a final step the output values are raised to power *p* in the conversion to firing rate *R*. Thus the model adopts the form of the 'contrast-gain/exponent model' (Albrecht & Geisler, 1991; Albrecht, Geisler, Frazor, & Crane, 2002), which in turn is similar to the 'half-squaring normalization model' (Heeger, 1992). Our model was elaborated to incorporate binocular summation and two stages of gain control (Truchard, Ohzawa, & Freeman, 2000), as well as the ocular dominance factor. Next we describe how this model structure was implemented and evaluated quantitatively.

2.3 Stage 1, nonlinear monocular responses and linear binocular combination

Fig. 2 sketches six ways in which the monocular gain controls might be organized, incorporating ipsiocular contrast gain control (CGC) and (optionally) interocular suppression (IOS). Both of these gain-control mechanisms can be driven by the current (test) contrast and the prior (adapting) contrast and these driving signals might arise *early* (before attenuation due to OD), or *late* (after OD attenuation).

For simplicity of description, but with no loss of generality, we assume throughout that for each cell the left eye is the more responsive one (dominant eye, DE) while the right eye is the less responsive (non-dominant eye, NE). Initial responses r_L, r_R in the monocular pathways leading to a given cortical cell, evoked by stimuli in the left and

right eyes (subscripted *L*, *R*), were defined by a modified Naka-Rushton function that contains extra terms representing the effect of prior adaptation to contrast in the same eye, and possible interocular suppression. We first outline the simplest model structure (Fig. 2C, model 3) here:

$$r_L = \frac{(1+s).S(\theta).d_L.c_L}{s + c_L + m.a_L} \qquad (1.3)$$

$$r_R = \frac{(1+s).S(\theta).d_R.c_R}{s + c_R + m.a_R} \qquad (2.3)$$

where *c* is test contrast, *a* is adapting contrast, *s* is the semi-saturation constant, *m* is the strength of contrast adaptation at this monocular level, d_L and d_R are attenuations of contrast due to OD ($d_L = 1, d_R \leq 1$), θ is the test orientation/direction relative to the preferred orientation of the cell, and $S(\theta)$ is the tuning function that attenuates these monocular responses by a fixed factor that depends only on test direction θ. The scale factor $(1+s)$ is a convenience, ensuring that the output is 1 for an input contrast of 1 at the preferred orientation with no adaptation. Orientation tuning is omitted from the denominator of eqns. 1.*x*, 2.*x* (where *x* is model number) because there is good evidence that the divisive gain control effect in V1 depends on stimulus contrast but shows little or no selectivity for orientation (Bonds, 1989), and that this is so because the divisive influence arises from a 'pool' of cells with many different preferred orientations and spatial frequencies (Carandini & Heeger, 2012; Heeger, 1992). The outcome is a 'contrast-set gain control' (Albrecht & Geisler, 1991; Geisler & Albrecht, 1992) rather than one in which gain depends directly on a cell's own response to a stimulus.

For all models, d_R attenuates the signal contrast (numerator in eqn. 2.3) but for early CGC it plays no part in setting the monocular gain *M* (determined by the denominator in eqn. 1.3, 2.3). With late CGC, however, the divisive term c_R is replaced by $c_R.d_R$, such that lower values of d_R reduce the divisive influence, and gain M_R increases for cells with greater ocular imbalance. This is analogous to the rise in monocular gain observed when contrast was decreased in one eye but not the other (Truchard et al, 2000; our Fig. 3). Note also that the empirical index for ocular dominance (ODI) is not the same as the model's dominance parameter *d*, though they are closely related. ODI is based on observed relative firing rates at the final output, while *d* is the hypothetical attenuation of one monocular input signal relative to the other ($d = d_R/d_L$) at an early stage (Fig. 1).

Evidence for interocular suppression (IOS) of responses r_L, r_R in the monocular pathways has frequently guided the design of binocular vision models (Ding & Sperling, 2006; Meese, Georgeson, & Baker, 2006; Moradi & Heeger, 2009; Wilson, 2017 for psychophysics; Sengpiel, Baddeley, Freeman, Harrad, & Blakemore, 1998; Sengpiel, Blakemore, & Harrad, 1995; Zhang et al., 2005 for physiology). IOS might seem irrelevant for the present dataset because the two eyes were never stimulated at the same time. But, potentially, adapting through one eye then testing the other might produce an adaptation effect via IOS, and so we incorporated IOS into the equations for models 1,2,4,5. See Appendix for a complete list of equations for all six models.

The six models (Fig. 2) differ only in the monocular gain control terms (denominator of eqns.1.*x*, 2.*x*) with no change in the numerator terms. The remaining definitions (eqns. 3,4,5 below) were common to all six models.

Monocular responses were a nonlinear function of contrast, but were summed linearly across the eyes to give the output r_B of stage 1:

$$r_B = r_L + r_R \qquad (3)$$

2.4 Stage 2, binocular adaptation and gain control

The final response $R(\theta)$ of a model cell as a function of test orientation is given in two parts by (i) a response function that incorporates divisive gain reduction by responses to both the current stimulus and to the previous adapting stimulus (r_B'):

$$R_B(\theta) = \frac{(1+z).r_B(\theta)}{1+z.e_B+b.r_B'} \qquad (4)$$

followed by (ii) an output nonlinearity and amplitude scaling:

$$R(\theta) = R_{max}.(R_B)^p \qquad (5)$$

where p, z and R_{max} are constants, b represents the strength of adaptation at the binocular level, and e_B represents the drive (if any) from the current stimulus into this second-stage gain control. See Appendix for further rationale and justification of these model steps.

2.5 The whole model

The model can be summarized by condensing eqns. 1-5 into a single equation (Fig. 1):

$$R = R_{max}.\{S(\theta).(c_L d_L M_L + c_R d_R M_R).B\}^p \qquad (6)$$

where (taking the right eye to be NE) we have d_L=1, d_R <= 1. Eqns. 1.*x*, 2.*x* operate as divisive, contrast-set gain controls, because the monocular gains (M_L,M_R, eqns. 7.*x*,8.*x*, Appendix) include a divisive term representing the test contrast (c_L or c_R). Likewise, the binocular gain B (eqn. 9, Appendix) includes the r_B term that represents short-term gain control at the binocular stage. Gain B is adapted (reduced) by previous binocular responses (r'_B) and (in principle) by the current response (r_B), if z>0. We fixed the values for s and z, guided by fitting eqns. 8.*x* and 9 to the gain values reported by Truchard *et al* (2000) for cat cortical cells (s=0.06, z=0; see legend to Fig. 3 for more detail). In particular, setting z=0 prevented any control of B gain by current contrast, in line with the Truchard *et al* findings.

*** Fig. 3 about here ***

2.6 Fitting the model

The fixed values adopted for s and z gave a typical, smoothly saturating contrast response (Albrecht and Geisler, 1991; Heeger, 1992; Carandini et al., 1997). And when z was a fitted parameter its value converged to zero, confirming that our *a priori* choice of z=0 was supported for this dataset. R_{max} was the observed peak firing rate for each cell group, but it played no part in the model-fitting of relative gain values. That left five parameters (m, b, p, w, d) to be assigned, but d was determined directly from the *unadapted* data alone without compromising the purpose of the model-fitting. See Appendix, eqns. 12, 13 for derivation of d.

We fitted model response gains to observed response gains (defined below) for the N OD cell groups simultaneously, using the method of least squares, with parameter adjustment implemented by the *Simplex* algorithm (*fminsearch* in *Matlab*). For each fitting, ten or more runs were done with jittered starting values of parameters to ensure that minimum-error solutions were not stuck in local minima. To keep the model as simple as possible (Occam's razor), and after some initial exploration, we assumed that the parameters m,b,p,w did not vary across the N OD groups. Thus there were 2-4 free parameters in the fitting, but 4N data points to be fitted (i.e. the N cell groups times the 4 adapting conditions whose data had not already been used in the determination of d).

*** Fig. 4 about here ***

3. Results

3.1 Overview of the cell response data

Figs. 4A,B give a summary of the physiological data, expressed as population means plotted against test orientation/direction. The descriptive tuning curve fitted to the unadapted DE data (Fig. 4A, black curve) also fitted closely to the unadapted NE data (Fig. 4B, black) and to the adapted responses of both eyes (coloured curves & symbols in Fig. 4A,B), subject only to a scaling-down of response magnitude that depended on which eye was adapted and which eye was tested, but was independent of test orientation. We refer to this scaling-down of the spike rates as a reduction in *response gain*, and we quantify these gains in Fig. 4C,D as the slope of the linear regression between responses in any given condition and those in the control condition (unadapted DE responses). If the tuning shape had changed markedly with adaptation, or between DE and NE, then the relations in Fig. 4C,D would not be linear, and our characterization in terms of response gain would be inappropriate. But as we shall see, this linearity held good not only for the population means but also quite well for sub-groups of cells with different degrees of OD, and this greatly simplified the analysis and modelling. Table 1 gives the gain factors (slopes in Fig. 4C,D) for the population mean data. Note that the gain factors describe relative responses only at the fixed high test contrast used in the experiment. Ocular dominance led to an average unadapted gain in the NE that was 43% of that in the DE.

Table 1. Response gains and firing rates for the population mean (54 cells)

	Response Gains, G		Firing rates, R_{max}, sp/s	
Adapt	Test DE	Test NE	Test DE	Test NE
None	1	0.430	36.1	14.9
NE	0.770	0.208	27.3	6.7
DE	0.359	0.227	12.3	8.5

In general, this population of cells showed interocular transfer (IOT) of contrast adaptation: adapting through one eye led to loss of response gain when testing the same eye or the other eye (Howarth et al., 2009). When the DE was tested, contrast adaptation in the same eye reduced gain much more than NE adaptation did (Fig.4C). But when the NE was tested, adaptation in either eye reduced gain by very similar amounts (Fig. 4D). This strong, asymmetric interaction cannot be described by any single figure-of-merit such as 'percentage interocular transfer'. Instead, our modelling aims to help us understand the basis for interocular transfer - in terms of gain changes at monocular and binocular levels of processing - and the influence that ocular dominance has on both contrast sensitivity and contrast adaptation.

*** Fig. 5 about here ***

3.2 Three OD groups

Next we illustrate the tuning and gain plots obtained when the cells were divided into different OD groups (see Methods). Figs. 5A,B show that the same orientation/direction tuning curve (the template in Fig. A1, blue) fitted very well in all 18 cases (6 conditions x 3 OD groups). The key point, though, is that the tuning shapes were sufficiently similar *within* each OD group that the responses mapped very well onto straight lines in Figs. 5C,D, thus defining a response gain for each condition (Table 2) with fairly high precision. Differences in tuning shape between OD groups would not affect these estimates of gain, but in practice we saw no dramatic differences in tuning, even with 9 or 10 groups.

Table 2. ODI and empirical response gains G for 3 OD groups (18 cells/gp)

	Group 1		Group 2		Group 3	
ODI	0.108		0.416		0.845	
	Response gains, G					
Adapt	Test DE	Test NE	Test DE	Test NE	Test DE	Test NE
None	1	0.095	1	0.378	1	0.787
NE	0.828	0.093	0.749	0.181	0.748	0.339
DE	0.374	0.002	0.336	0.194	0.376	0.449

3.3 Comparing models with data

Having established the appropriateness of these response gain measures, we now compare model gains with data, to assess the contributions made by different processing stages and to determine whether the evidence favours any particular model. The cells were divided into N groups and for each N the six model variants (Fig. 2) were fitted by least-squares to the cell gains determined for each group as described above. Goodness-of-fit was quantified by R^2, and we used AIC analysis (Burnham & Anderson, 2002; Wagenmakers & Farrell, 2004) for model comparison, to assess the relative strength of evidence (the *Akaike weight*) favouring each model. AIC is especially useful where models are not nested (where one model is not a special case of another) and a nested F-test cannot be use. See legend to Fig. 6 for more on AIC. Table 3 summarizes this analysis for $N = 3$, 6 and 9 OD groups. R^2 values were high for all 6 models, implying that all the models capture much of the observed variation in gain. Presumably this is so because all 6 models share the same general binocular architecture (Fig. 1). But that is *not* an indication that the evidence favours all the models equally. The AIC calculations in Table 3 show that model 5 (late CGC, early IOS) with high Akaike weights was consistently favoured over the others, though there was some support also for model 4. Fig. 6A plots the Akaike weights against model number, showing the high weight for model 5, and a modest weighting for model 4, irrespective of the number of cell groups from 3 to 10 (indicated by different colours and ordered from left to right for each model number).

438 **Table 3. Steps in AIC analysis for model comparison & model selection**
439

Model	R^2	K	SSerr	AICc	ΔAIC	Akaike weight
N groups = 3, n data = 12						
1. Early CGC, Late IOS	0.9756	5	0.0187	-57.56	14.040	0.001
2. Early CGC, Early IOS	0.9785	5	0.0165	-59.10	12.502	0.002
3. Early CGC, No IOS	0.9756	4	0.0187	-63.85	7.754	0.017
4. Late CGC, Late IOS	0.9896	5	0.0080	-67.80	3.797	0.122
5. Late CGC, Early IOS	**0.9924**	5	0.0058	-71.60	0.000	**0.811**
6. Late CGC, No IOS	0.9795	4	0.0157	-65.95	5.647	0.048
N groups = 6, n data = 24						
1. Early CGC, Late IOS	0.9552	5	0.0729	-125.77	12.369	0.002
2. Early CGC, Early IOS	0.9554	5	0.0726	-125.89	12.252	0.002
3. Early CGC, No IOS	0.9552	4	0.0729	-129.00	9.141	0.008
4. Late CGC, Late IOS	0.9694	5	0.0498	-134.94	3.206	0.162
5. Late CGC, Early IOS	**0.9732**	5	0.0436	-138.14	0.000	**0.807**
6. Late CGC, No IOS	0.9582	4	0.0681	-130.66	7.481	0.019
N groups = 9, n data = 36						
1. Early CGC, Late IOS	0.9362	5	0.1609	-182.77	12.554	0.001
2. Early CGC, Early IOS	0.9363	5	0.1606	-182.85	12.475	0.001
3. Early CGC, No IOS	0.9362	4	0.1609	-185.48	9.845	0.005
4. Late CGC, Late IOS	0.9520	5	0.1210	-193.03	2.300	0.235
5. Late CGC, Early IOS	**0.9550**	5	0.1135	-195.33	0.000	**0.742**
6. Late CGC, No IOS	0.9397	4	0.1521	-187.52	7.807	0.015

Notes:
No. of fitted parameters here was four (*m,b,p,w*), reducing to three for models 3 & 6 where *w*=0. In all later analyses, *p* was fixed at *p*=2.7; see legend to Fig. 6B.
The value K used in AIC is the no. of fitted parameters, plus 1.
Akaike weight can be interpreted as the probability that a given model is the best of those considered (Burnham & Anderson, 2002).

440

*** Fig. 6 about here ***

3.4 Choice of model parameters guided by contrast-response data

Inspection of the fitted parameters from this initial analysis revealed that for model 4 the output exponent p was surprisingly high (5.56±0.37, mean ± s.d. over the 8 levels of grouping). This was much higher than for model 5 (mean 2.98±0.19) as well as the other models, and also higher than many estimates of mean p in the physiological literature, eg. the canonical value of 2 required by energy models and half-squaring. In addition, having p as high as 5.5 renders the present models inconsistent with data on the contrast-response of cat V1 population means. Fig. 7 replots data from two extensive studies (Albrecht & Hamilton, 1982; Crowder, Van Kleef, Dreher, & Ibbotson, 2007) and there is good agreement between the two studies (done in different continents, 25 years apart), but poor agreement with the model's contrast response when p=5.5 (blue curve in Fig. 7). The best match between model and data here was given by p=2.7 (Fig. 7, red curve; R^2 = 0.966). Thus to make our models consistent with these data on unadapted contrast-responses, we fixed p=2.7, instead of making it a free parameter.

This choice of p gives the model contrast-response a semi-saturation contrast (c_{50}) of 0.20 in accord with the cat spike-rate data (Fig. 7). But now consider the contrast-response *before* the power transformation. In the model it is in essence a simple Naka-Rushton function of the form $r = c/(s+c)$, whose c_{50} is s, which we set to s = 0.06. This value is fairly close to the median c_{50} of 0.076 reported by Finn et al. (2007) (their Fig. 4F) for the membrane-potential responses of 46 cat cortical cells – and is 2-3 times lower than the c_{50} for spike rates (Fig. 7). This difference could arise directly from the output nonlinearity p. When we raise the early response r to the power p=*2.7* it is easy to calculate that this model 'spike-rate' transformation makes the contrast-response shallower and less compressive, and increases the c_{50} from 0.06 to 0.20, in line with the evidence just described. In short, two important fixed parameters s = 0.06, p = 2.7 are supported by evidence from contrast gains (Fig. 3), and from contrast-response functions at the level of membrane potential (Finn et al., 2007) and spike rates (Fig. 7).

*** Fig. 7 about here ***

3.5 The 'best' model

In AIC analysis, the Akaike weight estimates the probability that a given model is the best of those considered (Burnham & Anderson, 2002). With p fixed hereafter at p=2.7, we re-fitted the models and re-plotted the Akaike weights, as shown in Fig. 6B. Model 5 (late CGC, early IOS) was now uniquely favoured (mean weight = 0.935), while support for model 4 evaporated (mean weight = 0.029). Moreover, this pattern of Akaike weights remained very similar even when there was little or no averaging across cells. With 54, 27 or 18 groups (Fig. 6C) there were just 1, 2 or 3 cells per group respectively, and even though R^2 values decreased markedly in the absence of averaging, model 5 remained most likely to be the 'best' model as before (mean weight for model 5 = 0.90, model 4 = 0.06). The relative superiority of model 5 therefore cannot be attributed to any artefact of averaging across cells. See Table 4 for mean values of parameters in these model fittings. We turn now from model fitting to questions about the component processes underlying contrast adaptation.

Table 4. Best-fitting parameter values for models 1-6, with fixed p = 2.7

Model	s	z	b	m	p	w	
M1. Early CGC, Late IOS	0.06	0	0.182	0.475	2.7	0.000	mean
	-	-	*0.005*	*0.008*	-	*0.000*	*sd*
M2. Early CGC, Early IOS	0.06	0	0.178	0.482	2.7	0.010	mean
	-	-	*0.008*	*0.013*	-	*0.019*	*sd*
M3. Early CGC, No IOS	0.06	0	0.182	0.475	2.7	0	mean
	-	-	*0.005*	*0.008*	-	-	*sd*
M4. Late CGC, Late IOS	0.06	0	0.171	0.522	2.7	0.085	mean
	-	-	*0.007*	*0.009*	-	*0.007*	*sd*
M5. Late CGC, Early IOS	**0.06**	**0**	**0.096**	**0.691**	**2.7**	**0.141**	**mean**
	-	-	*0.015*	*0.030*	-	*0.012*	*sd*
M6. Late CGC, No IOS	0.06	0	0.203	0.458	2.7	0	mean
	-	-	*0.007*	*0.009*	-	-	*sd*

NOTES

1.Table shows mean and *SD* over the 8 cell groupings (*N*=3 to 10). Parameters *s,z,p* were fixed.
2. In practice, M1 = M3 because, after fitting, parameters *b,m,w* emerged as the same for both. Also, M2 was very close to M1,M3 in parameters and behaviour.

3.6 Is there any adaptation at the B level ?

We saw earlier (Fig. 3), that there appears to be little or no control of 'instantaneous' contrast gain at the binocular (*B*) level, an idea implemented here by z=0. Hence it is natural to ask whether the *B* level also has no contrast adaptation: does b=0 ? To answer this, we fitted models 1-6 as before, but with fixed b=0. We denote these modified versions as models 7-12 respectively. It might seem obvious that a cell with no adaptation at the binocular level (b=0) would not exhibit interocular transfer of adaptation, but that was true only for models 9 and 12 that had b=0 *and* lacked interocular suppression, ie. w=0. The model fits to cat response gains for these two models were very poor (eg. R^2 = 0.57, 0.58 for N=9) almost entirely because (unlike the cat cells) adapting one model eye had no effect at all on test responses through the other eye. But the question is less obvious for the other models (7,8,10,11) that did have interocular suppression. For models 7,8,11, but not 10, we found that increases in m and w (the IOS weight) largely but not entirely compensated for the lack of binocular-level adaptation. Interocular suppression, persisting from the adaptation period through to the test period, thus provides a plausible source of interocular transfer when *B* level adaptation is lacking. Nevertheless, from AIC analysis over the 12 models (Fig. 6D), we should still conclude that model 5 was the one best supported by the data while 'model 11' (ie. model 5 with b=0) received slight support. No others did.

Since M11 is nested within M5, we also used an F-test to determine whether M5 (with b as a free parameter) fitted significantly better than M11 (b=0). That is, did the inclusion of *B*-level adaptation in M5 justifiably improve the fit ? Table 5 suggests that it did. The mean P-value over the 8 cell groupings was 0.02, with median P = 0.01, and only one of 8 tests gave P>0.05. We should caution that the 8 tests were not independent, because they were based on the same raw data, albeit combined into groups differently in each case. Nevertheless, their consistency (7/8 tests gave P<0.05) reinforces the conclusion from AIC analysis: by including adaptation at the binocular level, model 5 accounts for the patterns of data better than models that do not.

F-test for nested models:

Table 5 Does M5 fit significantly better than M11?

Ngroups	F-ratio	Ndata	d.f.	Pvalue
3	12.791	12	1,9	0.005
4	5.733	16	1,13	0.031
5	6.541	20	1,17	0.020
6	8.941	24	1,21	0.007
7	6.71	28	1,25	0.016
8	3.311	32	1,29	0.079
9	9.944	36	1,33	0.003
10	12.719	40	1,37	0.001

Mean P-value over the 8 cell groupings = 0.020, median = 0.011

3.7 Is IOS a necessary feature of the model ?

We used the F-test again to ask whether IOS (with mean w=0.14, Table 4) contributed significantly to the fit of model 5. We did this by comparing M5 with M6 that did not include IOS (w=0). The answer from Table 6 is that all the P-values were very low (mean P = 0.0023, median 0.0014), thus strongly implying that IOS contributes significantly to the contrast adaptation effect. With IOS, adapting contrast in one eye drives down the gain of the other eye's monocular (M) mechanism, and some of that loss of gain persists to influence (reduce) the cell's later response to a test stimulus in the other eye.

F-test for nested models:

Table 6 Does M5 fit significantly better than M6?

Ngroups	F-ratio	Ndata	d.f.	Pvalue
3	15.931	12	1,9	0.0026
4	13.301	16	1,13	0.0026
5	16.031	20	1,17	0.0008
6	13.25	24	1,21	0.0014
7	8.056	28	1,25	0.0087
8	14.46	32	1,29	0.0007
9	12.113	36	1,33	0.0014
10	15.362	40	1,37	0.0004

Mean P-value over 8 cell groupings = 0.0023, median = 0.0014

3.8 Interim summary

Judged by R^2 values, all six models gave a good account of the Howarth *et al* (2009) dataset in terms of variance accounted for. For example, with N=6, R^2 was 0.955 or higher, both when p was fitted (Table 3) and when fixed (p=2.7). We think these fits are generally good because the models share the same basic structure and it is a useful one (Fig. 1). But R^2 is not a good tool for model comparison and model selection; small differences in R^2 can represent large differences in the extent to which one model should be preferred over another (Burnham & Anderson, 2002, pp. 95-96). For a more fine-grained comparison of the models, we used AIC analysis (Fig. 6) and found that model 5 was consistently the preferred model from this set of six models. The evidence supports the *late CGC, early IOS* scheme (Fig. 2E), such that adaptation occurs at both the M and

B levels, and interocular suppression contributes to adaptation at the *M* level. At the monocular (*M*) level, NE gain varies with OD, but DE gain does not. There is a significant contribution from adaptation at the binocular level though its strength is lower than in the other models (Table 4). Interocular transfer of adaptation is mediated by gain change at the binocular level and by the aftereffect of interocular suppression at the monocular level.

*** Fig. 8 about here ***

3.9 Trends in adapted gain as OD varied between groups

Fig. 8 plots cat response gains after adaptation (coloured symbols) as a function of OD, expressed as the ratio *D* of unadapted response gains (NE/DE) for each cell group. The unadapted response gains (grey squares) are important reference points, but not informative about the models because they are either 1.0 by definition (test DE) or are given from the data and choice of cell grouping, independently of any model (test NE). Each model should be assessed by how well it fits the *adapted* gains (red & cyan symbols).

Model 5 fitted the data very well for all 4 combinations of adapt eye and test eye (Fig. 8A,B,C, red & cyan; R^2=0.949, n=44 data). The simplest of the alternative models (M3) predicted adapted gains (black curves) that were almost identical to M5 when the adapted eye was tested (Fig. 8A,C), but showed clear deviations from the data in the between-eye conditions (cyan symbols) in two ways. (i) After NE adaptation, M3 predicted a fall in DE gain with increasing *D* (Fig. 8A, black curve) that was steeper than observed and steeper than predicted by M5 (cyan curve). (ii) After DE adaptation, M3 predicted higher NE test gains than observed over most of the range (Fig. 8B, black line). Model 5 (late CGC, early IOS) thus emerged as the preferred model overall, evident by inspection here and by the statistical analyses presented above (Fig. 6B,C & Tables 5,6; see also Fig. S8).

3.10 Monocular, binocular & interocular components of adaptation

To shed more light on underlying mechanisms, we consider model gain changes induced by adaptation at the *M* and *B* levels of processing. We begin with the simplest model M3 (Fig. 9) then consider how M5 adds extra insight (Fig. 10). [Note that models M1,2,3 are effectively the same here, because they differed only in IOS; model-fitting returned w=0 in all three cases, meaning that IOS was silenced and all three early CGC models were rendered equivalent.]

The largest effect of adaptation on cat cell response gains came from adapting and testing the dominant eye (which we denote here as DE/DE, meaning adapt DE/test DE): observed response gain fell from 1 to about 0.36, with no evident trend across the OD groups (Fig. 9D, red squares). M3 captured this effect through similar reductions of gain at the monocular level (gain 0.82, Fig. 9B, red) and at the binocular level (gain 0.85, Fig. 9C, red). Model response gain is the product of three factors ($d_L.M_L.B$), [1*0.82*0.85 = 0.70], raised to the power p, to give $(0.70)^{2.7}$ = 0.38, very close to the mean observed gain. Thus two small gain changes become a larger one because they are in series, and then the expansive nonlinearity amplifies the effect - smaller gains become even smaller. In *all* models there was no trend across the OD groups for this DE/DE condition, because any influence of OD is revealed only by stimulation of NE.

*** Figs. 9 & 10 about here ***

When the dominant eye was tested after non-dominant adaptation (NE/DE), cat response gain was reduced much less overall (Fig. 9D, cyan squares) and the reduction in gain tended to be greater with increasing ocular balance *D* of the cell group. The early CGC model (cyan curve) captured the reduced magnitude of the aftereffect but over-estimated

this downward trend across the OD groups. There was no IOS, and so in this interocular condition monocular gains were unchanged by adaptation (Fig. 9B, cyan), but NE adaptation scaled down binocular gain *B*. It did so just a little when *D* was close to 0 (Fig. 9C, cyan curve) because OD makes the adapting signal weak. When *D* is higher, *B* is scaled down more, because the adapting signal r_B' gets stronger as ocular balance approaches 1. But M3 consistently over-estimated this trend in the data, and because of their effective equivalence (noted above), M1 & M2 could do no better.

Model M5, on the other hand, was notably more accurate than M3 (Fig. 10D, or Fig. 8A, cyan curve). Early IOS reduced M_L uniformly over OD (Fig. 10B, cyan), and this gain change at the *M*-level meant that the predicted change of *B* gain was smaller (Fig. 10C), resulting in a shallower change in overall gain and a closer fit to the data (Fig. 10D or Fig. 8A, cyan). In brief, interocular suppression at the monocular level accounted for some of the interocular transfer of adaptation, while binocular-level adaptation accounted for the rest. Because the IOS component of this transfer was 'early', it was also uniform across OD, and so enabled M5 to account better for the shallowness of the trend in the data – a trend created at the *B* level of adaptation (Fig. 10C). The possibility of there being *no B*-level component of adaptation was considered but found little support (Table 5 & Fig. 6D).

Turning now to testing the non-dominant eye, we see a very different pattern of cell gains (Fig. 8B,C). Unadapted gains, by definition, increased across the OD groups (grey squares), and the observed aftereffects (reductions in gain) were of similar average magnitude after adapting the DE (Fig. 8B, cyan squares) or the NE (Fig. 8C, red squares). The simplest model M3 described the linear trend of these adapted gains fairly well (Fig. 9G, 9H), but exaggerated the difference in their slopes. Nevertheless, a fairly good model should be ousted by a better one, and that is so here: M5 has a much tighter fit to the DE/NE data (Fig. 8B, cyan), and to the NE/DE data (Fig. 8A, cyan). M5 also nicely captures the upward curvature in the DE/NE data (Fig. 8B or Fig. 10H, cyan), and the lack of it in the NE/NE data (Fig. 8C or Fig. 10G, red squares).

3.11 The 'signature' of the best-fitting model

To see why M5 behaves the way it does, we need to consider the adaptive changes in *M*- and *B*-gains across different OD groups. But in the late CGC models (M4,5,6) there are large increases in absolute M-gain with decreasing *D* (Fig. 10F) – a direct consequence of late, OD-dependent CGC that was not a feature of early CGC (Fig. 9F). To remove this trend and make it easier to see the *change* in gain due to adaptation, Figs. 11A and 11C plot the *gain ratio Q* (adapted *M* gain divided by unadapted *M* gain) as a function of *D*. Fig. 11A (test DE) is unaffected by this relative measure (since unadapted DE gain = 1), but Fig. 11C (test NE) now interestingly reveals that the predicted influence of OD on monocular gain change M_R is in *opposite* directions for DE adaptation (cyan) and NE adaptation (red). This crossover interaction carries through to the final plot of predicted response gain (Fig. 11D, thin curves) and is also evident in the cat data, where at low *D* the cyan symbols are mainly below the red but rise above at high values of *D*. The two predicted curves have opposite curvature, and track the corresponding data quite closely as *D* increases. When the number of cell groups was varied, a similar crossover in both data and model was seen in each case. Fig. S7, lower row, summarizes this for $N = 3,6,9$ groups.

*** Fig. 11 about here ***

We can think of this crossover (Fig. 11C,D) as the signature of models M5 (and M4), because it arises directly from the combination of *late* CGC and IOS (early or late). By our definition, *late* CGC is affected by OD (less NE/NE suppression when *D* is low) but

early CGC is not. For M5 and the same eye (NE/NE) condition we derive from eqn. 8.5 that with test contrast c_R=1 the adapted/unadapted M_R gain ratio Q_R is:

$$Q_R = \frac{s + d_R}{s + d_R + m.a_R.d_R}$$

where $m.a_R$ is constant and d_R increases with D (eqn. 13). When d_R is zero Q_R is 1, but then Q_R falls as d_R increases (red curve in Fig. 11C); adaptation here is least for the most unbalanced cells. But for DE adapt, NE test, adaptation at this monocular level depends on the interocular route, and from eqn. 8.5 we get:

$$Q_R = \frac{s + d_R}{s + d_R + m.w.a_L}$$

where $m.w.a_L$ is a positive constant. When d_R is zero $Q_R < 1$, but Q_R then *rises* towards 1 as d_R increases (cyan curve in Fig. 11C). In summary, this crossover can be seen as a defining characteristic of M5 – late CGC with early IOS – and its predictions are supported fairly clearly by the data (Fig. 11D).

Similar arguments apply for M4 (late CGC, late IOS) and a similar crossover occurs in its predictions for NE test (Fig. S4). But late IOS (M4) is influenced by OD while early IOS (M5) is not. This difference results in a poorer fit to the interocular NE/DE condition for M4 than M5 (Fig. S8G). Hence we continue to focus our attention on M5 as the best explanation within this set of models.

3.12 Number of OD groups

We wondered whether the pattern of observed effects (Fig.8) might depend on the way the cells were divided into groups, or on the size of the groups. But on close examination we did not see any notable variations in the pattern of experimental results or model behaviour across the different ways of grouping. The outcomes are summarized for M5 with N=3,6,9 in Fig. S7 (*Supplementary material*).

4. Discussion

We set out to increase our understanding of the functional architecture of binocular vision that allows cortical cells in V1 to respond to contrast, to adapt to contrast, and to combine inputs from the two eyes. The goal was to extend existing models by specifying how contrast adaptation may affect contrast gain both before and after binocular summation, and identifying where and how in this chain of events (Fig. 1) ocular dominance plays its part in making binocular cells less responsive to one eye than the other. To this end we re-analyzed and modelled data from Howarth et al. (2009), who studied contrast adaptation, interocular transfer, orientation/direction tuning and ocular dominance in cat cortical cells. To reduce variability and get a clearer picture of typical cell behaviour, we applied our models to responses averaged within subsets of cells that had similar degrees of ocular dominance (OD). An important simplification emerged: the orientation/direction tuning curve for these group-average responses had essentially the same shape for all OD groups and all the tested stimulus conditions, with or without adaptation of one or other eye. Adaptation, and ocular dominance, simply scaled all response rates down by a common factor which we call the *response gain*. A good model should therefore account for the pattern of changes in response gain, and maintain the tuning invariance, and strike a balance between simplicity and accuracy.

Using data and ideas from Truchard et al (2000), and from the extensive literature on suppressive gain controls, we devised simple expressions for monocular-level contrast gain controls (CGC) in which gain (for a given eye) might be driven down by the current test contrast and by prior adapting contrast in that eye or (to a lesser extent) the other eye.

Ocular dominance was represented by a single assumption - the contrast input to the non-dominant eye was attenuated by a fixed factor *d* that varied between cells, while input to the dominant eye was not influenced by OD. Indeed the model was simple and parsimonious, because the model cells were all the same except for the variation in dominance factor *d*. We used the model to derive *d* from the observed ratio *D* of unadapted gains in the two eyes. The cell response was shaped by the suppressive influences on the *M*-level CGC, arising either *early* (before OD) or *late* (after OD). Signals from the two eyes were then summed linearly and provided the excitatory drive for the cell, and the input to the binocular-level gain control. The final step, now standard in V1 models, was an accelerating power function nonlinearity, approximating the transformation from membrane potential to spike rate.

Our account proposes three sources of gain change underlying contrast adaptation: (i) monocular gain change induced directly for one eye when that eye was adapted, (ii) monocular gain change induced between-eyes by interocular suppression (IOS) that was driven by the adapter, and (iii) binocular gain change driven by previous levels of binocular response. We modelled six different ways in which these processes might be organized (Fig. 2), and fitted these models to sets of adapted response gains derived from data of 54 cells with a wide range of ODs. We found that just one model (M5, Fig. 2E) was consistently superior to the others. It combined *late* CGC with *early* IOS, meaning that ipsiocular gain change was influenced by OD, while interocular gain change via IOS at the monocular level was not. Adaptation at the binocular level was also present, but relatively small. This combination of characteristics explained (a) the slight, but not dramatic, dependence of interocular gain change on OD when the dominant eye was tested (Fig. 8A, cyan), (b) the complete lack of OD influence on ipsiocular gain change for the dominant eye (Fig. 8A, red), (c) the overall similarity between ipsi- and inter-ocular adapted gains when the non-dominant eye was tested (Fig. 11D), coupled with (d) the modest but consistent crossover interaction between OD and adapting eye, evident for both model gains and data in Fig. 11D. We showed that this interaction in the model (Fig. 11C) arose specifically from the combination of *late* CGC with IOS.

In short, a functional model (M5), with three sources of gain control (monocular, binocular, interocular) that has 3 corresponding fitted parameters (*m,b,w*) and 3 fixed parameters (*s,z,p*), gives us a compact and reasonably accurate account of the way ocular dominance influences contrast adaptation and interocular transfer across a heterogeneous sample of cells in cat visual cortex.

We showed that model M5 implies a significant role for gain change at the binocular level ($b>0$). This might suggest that contrast adaptation is somehow different from the 'instantaneous' contrast gain control studied by Truchard et al (2000), who found little or no evidence for binocular-level change in contrast gain. However, our analysis (Fig. 3) suggests a simpler resolution: in the stimulus conditions studied so far, changes of monocular gain can be large, while binocular gain changes are relatively small, but not negligible. Further experimental studies comparing the characteristics of simultaneous and successive changes in contrast gain would be valuable.

4.1 Limitations and efforts to overcome them

• In the experiments re-analyzed here, adapting and test contrasts were fixed at a single value, and so important features of the proposed gain controls remained untested. In part we filled the gaps by ensuring that each model's monocular contrast gains closely matched the contrast-dependence of gain measurements made by Truchard et al (2000) (Fig. 3). We also ensured good agreement between the model's unadapted contrast response function and population data from two other studies (Fig. 7).

• Adapting and test stimuli were always monocular. From the models we found that changes in gain due to adaptation were expected to be present at early (monocular) and later (binocular) levels (Figs. 9B,C, 10B,C). The exception was that when OD was extreme (*D* close to 0) adapting the non-dominant eye gave little change of response gain (in both model and data; Figs. 9D,10D). This was well explained by the attenuating effect of OD on the binocular-level response to the adapter. An obvious limitation, though, is that this model for responses of binocular cells has not been challenged with binocular or dichoptic stimuli. More evidence is needed, especially by combining contrast adaptation with simultaneous, dichoptic testing of both eyes.

We aim to address some of these issues in future work by comparing model performance with published data from cat cortical responses to binocular gratings that differed in contrast and/or phase between the eyes (Freeman & Robson, 1982; Kara & Boyd, 2009; Ohzawa & Freeman, 1986; Smith, Chino, Ni, & Cheng, 1997; Smith, Chino, Ni, Ridder, et al., 1997; Truchard et al., 2000), briefly discussed next.

4.2 Disparity sensitivity, CGC, and compensation for OD

When V1 cells are tested with the same sinewave gratings drifting in the same direction in both eyes, their response often varies with the phase disparity ϕ between the eyes. The response is modulated by disparity and the depth of modulation, known as the *binocular interaction index* (BII), is a single number that quantifies the disparity sensitivity of the cell. If left and right eye responses were proportional to contrast, and then summed, the response over disparity would, as observed, be deeply modulated when the input contrasts were equal. But if one eye's contrast were reduced its influence on the binocular sum would decrease, and the BII would fall markedly as the two contrasts became more unequal. Surprisingly, however, the BII for cells in both cat and monkey visual cortex tended to be fairly constant as the interocular contrast ratio varied (Freeman & Ohzawa, 1990; Smith, Chino, Ni, & Cheng, 1997), implying some important nonlinearity in the monocular input paths (Freeman & Ohzawa, 1990).

Truchard *et al* (2000) resolved this question by showing that monocular gain controls compensate for differences in contrast between the eyes. Such cells might encode disparity without being perturbed by contrast mismatch. Freeman & Ohzawa (1990) were the first to report evidence of this kind, and they conjectured that "ocular dominance may be compensated for by such a mechanism under binocular viewing conditions". From our modelling we can take this a step further: compensation for OD occurs with *late* CGC but not early CGC. Fig. 12A shows how with early CGC the NE response is strongly attenuated (relative to DE) by factor *d* at all contrasts (green curve). But with late CGC the attenuation is much less than factor *d*, implying a substantial degree of compensation for OD (red curve). Why is the attenuation less ? With late CGC the divisive signal is *d.c* (not *c*) and so there is less suppression as *d* gets lower. Hence monocular gain rises (cf. Fig. 10F) and this partly compensates for the signal attenuation due to OD, as Fig. 12 shows (red *vs* green curves). This suggests an important functional role for late CGC in (partially) compensating for OD, making the inputs to binocular summation more balanced than they otherwise would be. That in turn should increase the disparity sensitivity (BII) of the cell, as it does when contrasts are physically mismatched between the eyes (Truchard et al, 2000).

*** Fig. 12 about here ***

4.3 Importance of the saturation constant, s

Many or most V1 cells respond nonlinearly to contrast (e.g. Fig. 7), but some respond more linearly. For example, (i) Albrecht et al (2002) reported that in their study and others about 5% of V1 cells "demonstrated a nearly linear relationship" between response and

contrast, and (ii) some cells in monkey V1 showed linear binocular summation contours (Smith, Chino, Ni, & Cheng, 1997, their Figs. 6-12). The latter result requires both a linear contrast response in each monocular pathway, and linear binocular summation of those responses. The linear monocular contrast response in these cases (i and ii) can be modelled by increasing the saturation constant *s* to about 1.0 or higher. The finding of different degrees of linearity across cells thus suggests non-trivial variations of *s* in the V1 population. Indeed, recent recordings in cat cortex suggest that the degree of contrast-response nonlinearity is another property that is systematically mapped across the cortex. Cells near pinwheel centres were close to linear, while those in the iso-orientation domains (away from pinwheel centres) "ranged from almost linear to almost perfectly compressive" (Koch, Jin, Alonso, & Zaidi, 2016). We therefore expect such cells also to vary in how they handle binocular combination.

5. Conclusions

The statistician George Box famously wrote that "All models are wrong, but some are useful". He expanded on this memorable one-liner (see *Wikipedia*, 'All models are wrong') to indicate that, because all models are approximations, the only question of interest is: "Is the model illuminating and useful?". We think the present model M5 (Fig. 2E) is both useful and illuminating. It synthesizes several established concepts and mechanisms in a new way. We tested it against a key set of physiological results, and the outcome gave support to the general model structure (Fig. 1) and a particular form of it (Fig. 2E). It allowed us:

(i) to tease apart the contributions made to contrast adaptation in V1 cells by gain change at monocular and binocular levels of processing;

(ii) to identify a probable contribution from interocular suppression to monocular-level adaptation and gain change;

(iii) to make specific proposals about how ocular dominance operates in relation to CGC and IOS that account more accurately for the different patterns of adapted response gain observed when the dominant and non-dominant eyes were tested; and

(iv) to show that a functional advantage of *late* CGC is that it partly compensates for the imbalance of binocular inputs induced by ocular dominance.

§§§§§§§§§§§§§§§§§§§§

Appendix

Equations for the six models

Fig. 2 sketched six ways in which the monocular gain controls might be organized, incorporating ipsiocular contrast gain control (CGC) and (optionally) interocular suppression (IOS). We suppose that both these gain-control mechanisms can be driven by both the current (test) contrast and the prior (adapting) contrast and that these driving signals might arise *early* (before attenuation due to OD), or *late* (after OD attenuation). First, we specify models 3,2,1 that have early CGC. We begin with the simplest model (M3), and build from there.

Model 3: Early CGC, no IOS

Monocular responses r_L, r_R to a stimulus with contrasts c_L, c_R are:

$$r_L = \frac{(1+s).S(\theta).d_L.c_L}{s + c_L + m.a_L} \qquad (1.3)$$

$$r_R = \frac{(1+s).S(\theta).d_R.c_R}{s + c_R + m.a_R} \qquad (2.3)$$

where *L* and *R* subscripts refer to left and right eyes, *c* is test contrast, *a* is adapting contrast, d_L and d_R are the attenuation factors related to ocular dominance, *s* is a semi-saturation constant, *m* is the strength parameter for contrast adaptation at this monocular level, θ is the test orientation/direction relative to the preferred orientation of the cell, and $S(\theta)$ is the orientation sensitivity curve. Note that by our definition of *early* CGC the divisor (gain control) terms are not affected by the ocular dominance factors. The numerator - a linear response to contrast - is scaled by both *S* and *d* terms and is the same for all models.

Model 2: Early CGC, early IOS

$$r_L = \frac{(1+s).S(\theta).d_L.c_L}{s + c_L + w.c_R + m.(a_L + w.a_R)} \qquad (1.2)$$

$$r_R = \frac{(1+s).S(\theta).d_R.c_R}{s + c_R + w.c_L + m.(a_R + w.a_L)} \qquad (2.2)$$

With IOS, left eye contrasts reduce the gain for right eye responses, and vice-versa. The IOS terms (*w.c, w.a*) have been introduced 'early', without scaling by d_L or d_R. Parameter *w* is the weight factor for IOS.

Model 1: Early CGC, late IOS

$$r_L = \frac{(1+s).S(\theta).d_L.c_L}{s + c_L + w.c_R.d_R + m.(a_L + w.a_R.d_R)} \qquad (1.1)$$

$$r_R = \frac{(1+s).S(\theta).d_R.c_R}{s + c_R + w.c_L.d_L + m.(a_R + w.a_L.d_L)} \qquad (2.1)$$

Interocular suppression terms ($w.c_R.d_R$, $w.a_R.d_R$, etc) have been introduced 'late', hence scaled by the OD factors d_L, d_R.

Model 6: Late CGC, no IOS

We now describe the corresponding equations for *late* CGC, models 6,5,4, beginning with the simplest (M6). Monocular responses r_L, r_R to a stimulus with contrasts c_L, c_R are:

$$r_L = \frac{(1+s).S(\theta).d_L.c_L}{s + c_L.d_L + m.a_L.d_L} \qquad (1.6)$$

$$r_R = \frac{(1+s).S(\theta).d_R.c_R}{s + c_R.d_R + m.a_R.d_R} \qquad (2.6)$$

Model 5: Late CGC, early IOS

$$r_L = \frac{(1+s).S(\theta).d_L.c_L}{s + c_L.d_L + w.c_R + m.(a_L.d_L + w.a_R)} \qquad (1.5)$$

$$r_R = \frac{(1+s).S(\theta).d_R.c_R}{s + c_R.d_R + w.c_L + m.(a_R.d_R + w.a_L)} \qquad (2.5)$$

In eqn. 1.5, CGC terms ($c_L.d_L$, $a_L.d_L$) are late, while IOS terms ($w.c_R$, $w.a_R$) are early and similarly for eqn 2.5 (but with L,R swapped).

Model 4: Late CGC, late IOS

Finally, equations for late CGC, late IOS contain all possible gain terms in our scheme:

$$r_L = \frac{(1+s).S(\theta).d_L.c_L}{s + c_L.d_L + w.c_R.d_R + m.(a_L.d_L + w.a_R.d_R)} \qquad (1.4)$$

$$r_R = \frac{(1+s).S(\theta).d_R.c_R}{s + c_R.d_R + w.c_L.d_L + m.(a_R.d_R + w.a_L.d_L)} \qquad (2.4)$$

The six models here are different only in the gain control (denominator terms) with no change in the numerator terms.

Binocular summation

After equations 1.*x*, 2.*x*, (where *x* is model number) the remaining definitions (eqns. 3,4,5,6) are common to all six models. Responses to the two eyes are linearly summed:

$$r_B = r_L + r_R \qquad (3).$$

Responses to the adapter

From eqns 1-3, we can also describe Stage 1 responses *r′ during* the adaptation period where there is no prior adaptation term, and the current contrast is a_L rather than c_L. We illustrate model 4 here; the others should be obvious.

$$r'_L = \frac{(1+s).S(\theta).d_L.a_L}{s + a_L.d_L + w.a_R.d_R} \qquad (1'.4)$$

$$r'_R = \frac{(1+s).S(\theta).d_R.a_R}{s + a_R.d_R + w.a_L.d_L} \qquad (2'.4)$$

$$r'_B = r'_L + r'_R \qquad (3')$$

where $S(\theta) = 1$, because the adapter was always at the cell's preferred orientation.

Stage 2, binocular adaptation and gain control

Much psychophysical evidence (e.g. Baker & Meese, 2012; Bjørklund & Magnussen, 1981; Blake, Overton, & Lema-Stern, 1981; Vilidaitė & Baker, 2015) and a smaller number of physiological studies (Howarth et al., 2009; Maffei, Fiorentini, & Bisti, 1973) have shown that contrast adaptation transfers, at least partially, from adapting one eye to testing the other. Hence some component of adaptation is likely to lie at or after the point of binocular combination, and Stage 2 of this model represents contrast adaptation at the level of binocular integration. The final response $R(\theta)$ of a model cell as a function of test orientation is given in two parts by (i) a response function that incorporates divisive gain reduction by responses to both the current stimulus and the previous adapting stimulus:

$$R_B(\theta) = \frac{(1+z).r_B(\theta)}{1+z.e_B+b.r'_B} \qquad (4)$$

followed by (ii) an output nonlinearity and amplitude scaling:

$$R(\theta) = R_{max}.(R_B)^p \qquad (5)$$

where p, z and R_{max} are constants, b represents the strength of adaptation at the binocular level, and e_B represents the drive from the current stimulus into this second-stage gain control. Normalization models (e.g. Heeger, 1992; reviewed by Carandini & Heeger, 2012; Sawada & Petrov, 2017) typically suppose that e_B is an amalgam of responses from many nearby cells (the 'normalization pool'). An important feature is that e_B should depend on contrast but be invariant with stimulus orientation, in order that the orientation tuning is preserved over different contrast levels, as observed physiologically (Albrecht and Geisler, 1991; Heeger, 1992; Carandini et al., 1997; Scholl, Latimer, & Priebe, 2012). Pooling signals from many cells of different preferred orientations is a way to achieve that invariance, but a simple near-equivalent for our model was to assume that $e_B = max(r_B(\theta))$. The value of z controls the strength of this gain control effect, and the $(1+z)$ term on the numerator ensures that R_B is 1 when r_B is 1 in the absence of adaptation. It follows that (for monocular stimuli, as here) the peak final output $R = R_{max}$ when $R_B = e_B = r_B = c_L = 1$, irrespective of p. Importantly, when $b>0$, some trace of the previous response r'_B to the adapter acts to drive down the gain of the current response R_B to the test. Gain change at this binocular level, and/or interocular suppression at the monocular level, could mediate interocular transfer of adaptation.

Output transducer

Squaring of the output values (p=2) is a default assumption in some cortical cell models (Heeger, 1992), but physiological studies broadly agree that the value of p varies quite widely across V1 cells from about 1 to 5, with a cat population mean ± SD of about 2.5 ± 1.35 (Albrecht & Hamilton, 1982). The weight of physiological evidence favouring a power-law output nonlinearity (Albrecht & Geisler, 1991; Contreras & Palmer, 2003; Priebe, 2008; Priebe & Ferster, 2005; Priebe, Mechler, Carandini, & Ferster, 2004; Sclar, Maunsell, & Lennie, 1990) led us first to fit the model with p as a free parameter. In section 3.4 we give reasons why an *apriori* value of p (p = 2.7, determined by other published data) is more appropriate.

Monocular & Binocular gains

The whole model can be summarized by condensing eqns. 1-5 into a single equation (Fig. 1):

$$R = R_{max}.\{S(\theta).(c_L d_L M_L + c_R d_R M_R).B\}^p \qquad (6)$$

The monocular gain factors in eqn. 6 are obtained from eqns. 1.*x*, 2.*x* by deleting the *S,d,c* terms in the numerator. For example, in model 4:

$$M_L = (1+s)/(s+c_L.d_L+w.c_R.d_R+m.(a_L.d_L+w.a_R.d_R)), \qquad (7.4)$$

$$M_R = (1 + s)/(s + c_R.d_R + w.c_L.d_L + m.(a_R.d_R + w.a_L.d_L)), \quad (8.4)$$

or model 5:

$$M_L = (1 + s)/(s + c_L.d_L + w.c_R + m.(a_L.d_L + w.a_R)), \quad (7.5)$$

$$M_R = (1 + s)/(s + c_R.d_R + w.c_L + m.(a_R.d_R + w.a_L)). \quad (8.5)$$

B is obtained for all models by deleting r_B from the numerator in eqn. 4:

$$B = (1 + z)/(1 + z.max(r_B) + b.r'_B), \quad (9)$$

and d_L=1, d_R <= 1.

Deriving dominance parameter d from unadapted data

The dominance ratio parameter d was derived from the unadapted data, as follows. In general, from eqn. 6 the spike-rate response to monocular contrast c in the left eye (c_L=c, c_R=0) is:

$$R_L = R_{max}.\{S(\theta).(cd_LM_L).B\}^p \quad (10)$$

and similarly for contrast in the right eye (c_R=c, c_L=0):

$$R_R = R_{max}.\{S(\theta).(cd_RM_R).B\}^p \quad (11).$$

With early CGC (models 1-3) inspection of eqns. 7,8,9 shows that in the absence of adaptation (a_L = 0, a_R = 0) M_L (in eqn. 10) and M_R (in eqn. 11) are equal, and given that z=0 the gain B is also the same for these two monocular inputs. If we now take their spike-response ratio R_R/R_L, all but the d_L, d_R terms cancel out. Simple manipulation thus reveals that, for any test contrast and orientation, the response ratio $R_R/R_L = \{d_R/d_L\}^p$. By definition $d = d_R/d_L$, and so the dominance factor d is the spike-rate response ratio, 'back-projected' through the output nonlinearity: $d = \{R_R/R_L\}^{1/p}$. In practice, the most reliable way to exploit this relation was to work with the unadapted response *gains* G_{NE}, G_{DE} (slopes of the kind seen in Fig. 4C,D, black) because they made best use of the response data from all test orientations. Using these empirical unadapted gains of each OD cell group, and letting $D = G_{NE}/G_{DE}$ we computed

$$d = D^{1/p} \quad (12).$$

For late CGC (models 4-6), the factor d for each OD group could again be derived from the unadapted data via the model equations, but now depended on s and c as well as p:

$$d = \frac{s.D^{1/p}}{s + c.(1 - D^{1/p})} \quad (13),$$

where c is the fixed test contrast at which the unadapted data were collected.

*** Fig. A1 about here ***

Orientation/direction tuning

The tuning curve $S(\theta)$ was derived by first fitting a function $r(\theta)$ to the population-mean (unadapted) DE response data, and then normalizing it. The fitted function $r(\theta)$ (Fig. A1, blue curve) had a Gaussian central lobe in the preferred direction (θ=0), and a similar lobe of lower amplitude in the non-preferred direction (Carandini & Ferster, 2000; Gardner, Anzai, Ohzawa, & Freeman, 1999). It was defined over the range -180 <= θ <= 180 as:

$$r(\theta) = r_0.\left\{\alpha + exp\left(\frac{-\theta^2}{2\sigma^2}\right) + \beta.exp\left(\frac{-(\theta - 180)^2}{2\sigma^2}\right) + \beta.exp\left(\frac{-(\theta + 180)^2}{2\sigma^2}\right)\right\} \quad (14)$$

where θ is the orientation/direction of the moving test stimulus in degrees, α was a small upward offset of the whole tuning curve, σ represents orientation bandwidth, β describes direction selectivity as the relative amplitude of response in the non-preferred direction (θ=±180^{O}) and r_0 is a scale factor. There was a very close fit (R^2 = 0.999) of this descriptive function to the unadapted DE response (Fig. A1, circles, average of all 54 cells). Best-fitting tuning parameters were: α = 0.145, β = 0.501, σ = 23.0^{O} and r_0 = 31.5 spikes/s, corresponding to a peak rate r_{max} of 36.1 spikes/s. These values were used to create the tuning curve *S(θ)* for the model, normalized to a peak of 1:

$$S(\theta) = \{r(\theta)/r_{max}\}^{1/p}$$

where the power (1/*p*) compensates for the fact that the spike-rate data to which *r*(θ) is fitted are observed *after* the output nonlinearity, while the tuning curve *S* in the model lies before it. It is now well-established that the selectivity of cortical neurons is sharpened by an expansive output nonlinearity (Albrecht & Geisler, 1991; Anderson, 2000; Carandini & Ferster, 2000; Heeger, 1992; Miller & Troyer, 2002). Because the exponent *p* is greater than 1, *S* is broader and with a higher baseline than the observed response tuning *r*, as Fig. A1 shows (cf. Finn, Priebe, & Ferster, 2007, their Fig. 1) .

Tuning parameters for population-mean unadapted NE responses (α = 0.181, β = 0.512, σ = 24.6 ^{O}) were very similar to those for DE given above, and the tuning parameters α, β, σ varied very little with adapting condition, most likely because the adapter was always at the preferred orientation of the cell. Adapting to non-preferred orientations is known to have complex effects on both orientation tuning and bandwidth (Crowder et al., 2006; Dragoi, Sharma, & Sur, 2000; Patterson et al., 2013) outside the scope of the present work.

==========

References

Albrecht, D G, & Hamilton, D. B. (1982). Striate cortex of monkey and cat: Contrast response function. *Journal of Neurophysiology*, *48*(1), 217–237. https://doi.org/10.1152/jn.1982.48.1.217

Albrecht, D G., & Geisler, W. S. (1991). Motion selectivity and the contrast-response function of Simple cells In the visual cortex. *Visual Neuroscience*, *7*(6), 531–546. https://doi.org/10.1017/S0952523800010336

Albrecht, D G., Geisler, W. S., Frazor, R. A., & Crane, A. M. (2002). Visual cortex neurons of monkeys and cats: Temporal dynamics of the contrast response function. *Journal of Neurophysiology*, *88*(2), 888–913. https://doi.org/10.1152/jn.2002.88.2.888

Albrecht, D G, Farrar, S. B., & Hamilton, D. B. (1984). Spatial contrast adaptation characteristics of neurones recorded in the cat's visual cortex. *Journal of Physiology*, *347*, 713–739.

Anderson, J. S. (2000). The Contribution of Noise to Contrast Invariance of Orientation Tuning in Cat Visual Cortex. *Science*, *290*(5498), 1968–1972. https://doi.org/10.1126/science.290.5498.1968

Anzai, A, Ohzawa, I., & Freeman, R. D. (1997). Neural mechanisms underlying binocular fusion and stereopsis: position vs. phase. *Proceedings of the National Academy of Sciences*, *94*(May), 5438–5443. https://doi.org/10.1073/pnas.94.10.5438

Anzai, A, Ohzawa, I., & Freeman, R. D. (1999a). Neural mechanisms for encoding binocular disparity: receptive field position versus phase. *Journal of Neurophysiology*, *82*(510), 874–890.

Anzai, A, Ohzawa, I., & Freeman, R. D. (1999b). Neural mechanisms for processing binocular information II. Complex cells. *Journal of Neurophysiology*, *82*(510), 909–924.

Anzai, A, Ohzawa, I., & Freeman, R. D. (1999). Neural mechanisms for processing binocular information. I. Simple cells. *Journal of Neurophysiology*, *82*(2), 891–908. https://doi.org/10.1152/jn.1999.82.2.891

Baker, D. H., & Meese, T. S. (2012). Interocular transfer of spatial adaptation is weak at low spatial frequencies. *Vision Research*, *63*, 81–87. https://doi.org/10.1016/j.visres.2012.05.002

Barlow, H. B., Blakemore, C., & Pettigrew, J. D. (1967). The neural mechanism of binocular depth discrimination. *Journal of Physiology*, *193*, 327–342.

Bjørklund, R. A., & Magnussen, S. (1981). A study of interocular transfer of spatial adaptation. *Perception*, *10*(5), 511–518.

Blake, R., Overton, R., & Lema-Stern, S. (1981). Interocular transfer of visual aftereffects. *Journal of Experimental Psychology. Human Perception and Performance*, *7*(2), 367–381.

Blakemore, C. B., & Campbell, F. W. (1969). On the existence of neurones in the human visual system selectively sensitive to the orientation and size of retinal images. *Journal of Physiology*, *203*, 237–260.

Bonds, A. B. (1989). Role of inhibition in the specification of orientation selectivity of cells in the cat striate cortex. *Visual Neuroscience*, *2*(1), 41–55. https://doi.org/10.1017/S0952523800004314

Bonds, A. B. (1991). Temporal dynamics of contrast gain in single cells of the cat striate cortex. *Visual Neuroscience*, *6*(3), 239–255. https://doi.org/10.1017/S0952523800006258

Burnham, K. P., & Anderson, D. R. (2002). *Model selection and multimodel inference* (2nd ed.). New York: Springer.

Carandini, M, & Ferster, D. (2000). Membrane potential and firing rate in cat primary visual cortex. *The Journal of Neuroscience*, *20*(1), 470–484.

Carandini, M, & Heeger, D. J. (2012). Normalization as a canonical neural computation.

Nature Reviews. Neuroscience, *13*(1), 51–62. https://doi.org/10.1038/nrn3136
Contreras, D., & Palmer, L. (2003). Response to contrast of electrophysiologically defined cell classes in primary visual cortex. *The Journal of Neuroscience*, *23*(17), 6936–6945. https://doi.org/10.1523/JNEUROSCI.23-17-06936.2003
Crowder, N. A., Price, N. S. C., Hietanen, M. A., Dreher, B., Clifford, C. W. G., & Ibbotson, M. R. (2006). Relationship between contrast adaptation and orientation tuning in V1 and V2 of cat visual cortex. *Journal of Neurophysiology*, *95*(1), 271–283. https://doi.org/10.1152/jn.00871.2005
Crowder, N. A., Van Kleef, J., Dreher, B., & Ibbotson, M. R. (2007). Complex cells increase their phase sensitivity at low contrasts and following adaptation. *Journal of Neurophysiology*, *98*(3), 1155–1166. https://doi.org/10.1152/jn.00433.2007
Ding, J., & Sperling, G. (2006). A gain-control theory of binocular combination. *Proceedings of the National Academy of Sciences*, *103*(4), 1141–1146. https://doi.org/10.1073/pnas.0509629103
Dragoi, V., Sharma, J., & Sur, M. (2000). Adaptation-induced plasticity of orientation tuning in adult visual cortex. *Neuron*, *28*(1), 287–298. https://doi.org/10.1016/S0896-6273(00)00103-3
Finn, I. M., Priebe, N. J., & Ferster, D. (2007). The emergence of contrast-invariant orientation tuning in simple cells of cat visual cortex. *Neuron*, *54*(1), 137–152. https://doi.org/10.1016/j.neuron.2007.02.029
Freeman, R.D., & Robson, J. G. (1982). A new approach to the study of binocular interaction in visual cortex: Normal and monocularly deprived cats. *Experimental Brain Research*, *48*, 296–300.
Freeman, R D, & Ohzawa, I. (1990). On the neurophysiological organization of binocular vision. *Vision Research*, *30*(11), 1661–1676.
Gardner, J. L., Anzai, A., Ohzawa, I., & Freeman, R. D. (1999). Linear and nonlinear contributions to orientation tuning of simple cells in the cat's striate cortex. *Visual Neuroscience*, *16*(6), 1115–1121. https://doi.org/10.1017/S0952523899166112
Geisler, W. S., & Albrecht, D. G. (1992). Cortical Neurons: Isolation of Contrast Gain Control. *Vision Research*, *32*(8), 1409–1410.
Georgeson, M. A., & Georgeson, J. M. (1987). Facilitation and masking of briefly presented gratings: time-course and contrast dependence. *Vision Research*, *27*(3), 369–379.
Georgeson, M. A., & Harris, M. G. (1984). Spatial selectivity of contrast adaptation: Models and data. *Vision Research*, *24*(7). https://doi.org/10.1016/0042-6989(84)90214-1
Greenlee, M. W., Georgeson, M. A., Magnussen, S., & Harris, J. P. (1991). The time course of adaptation to spatial contrast. *Vision Research*, *31*(2), 223–236. https://doi.org/10.1016/0042-6989(91)90113-J
Heeger, D J. (1992). Half-squaring in responses of cat striate cells. *Visual Neuroscience*, *9*, 427–443.
Heeger, D J. (1992). Normalization of cell responses in cat striate cortex. *Visual Neuroscience*, *9*, 181–197. https://doi.org/10.1017/S0952523800009640
Howarth, C. M., Vorobyov, V., & Sengpiel, F. (2009). Interocular transfer of adaptation in the primary visual cortex. *Cerebral Cortex*, *19*(8), 1835–1843. https://doi.org/10.1093/cercor/bhn211
Hubel, D. H., & Wiesel, T. N. (1962). Receptive fields, binocular interaction and functional architecture in the cat's visual cortex. *Journal of Physiology*, *160*, 106–154.
Hubel, D. H., & Wiesel, T. N. (1968). Receptive fields and functional architecture of monkey striate cortex. *Journal of Physiology*, *195*, 215–243.
Kara, P., & Boyd, J. D. (2009). A micro-architecture for binocular disparity and ocular dominance in visual cortex. *Nature*, *458*(7238), 627–631. https://doi.org/10.1167/7.15.21

Koch, E., Jin, J., Alonso, J. M., & Zaidi, Q. (2016). Functional implications of orientation maps in primary visual cortex. *Nature Communications*, *7*, 1–13. https://doi.org/10.1038/ncomms13529

Maffei, L., Fiorentini, A., & Bisti, S. (1973). Neural Correlate of Perceptual Adaptation to Gratings. *Science*, *182*(4116), 1036–1038.

Marr, D., & Poggio, T. (1979). A computational theory of human stereo vision. *Proceedings of the Royal Society B: Biological Sciences*, *204*, 301–328.

Meese, T.S., Georgeson, M. A., & Baker, D. H. (2006). Binocular contrast vision at and above threshold. *Journal of Vision*, *6*(11). https://doi.org/10.1167/6.11.7

Meese, T S, & Hess, R. F. (2004). Low spatial frequencies are suppressively masked across spatial scale, orientation, field position, and eye of origin. *Journal of Vision*, *4*, 843–859. https://doi.org/10.1167/4.10.

Miller, K. D., & Troyer, T. W. (2002). Neural noise can explain expansive, power-law nonlinearities in neural response functions. *Journal of Neurophysiology*, *87*(2), 653–659.

Moradi, F., & Heeger, D. J. (2009). Inter-ocular contrast normalization in human visual cortex. *Journal of Vision*, *9(3):13*, 1–22. https://doi.org/10.1167/9.3.13

Ohzawa, I., Sclar, G., & Freeman, R. D. (1985). Contrast gain control in the cat's visual system. *Journal of Neurophysiology*. https://doi.org/10.1152/jn.1985.54.3.651

Ohzawa, I. (1998). Mechanisms of stereoscopic vision: the disparity energy model. *Current Opinion in Neurobiology*, *8*(4), 509–515.

Ohzawa, I, & Freeman, R. D. (1986). The binocular organization of simple cells in the cat's visual cortex. *Journal of Neurophysiology*, *56*(1), 221–242.

Ohzawa, I, DeAngelis, G. C., & Freeman, R. D. (1990). Stereoscopic depth discrimination in the visual cortex: neurons ideally suited as disparity detectors. *Science*, *249*, 1037–1041.

Ohzawa, I, DeAngelis, G. C., & Freeman, R. D. (1996). Encoding of binocular disparity by simple cells in the cat's visual cortex. *Journal of Neurophysiology*, *75*(5), 1779–1805.

Patterson, C. A., Wissig, S. C., & Kohn, A. (2013). Distinct effects of brief and prolonged adaptation on orientation tuning in primary visual cortex. *Journal of Neuroscience*, *33*(2), 532–543. https://doi.org/10.1523/JNEUROSCI.3345-12.2013

Pettigrew, J. D., Nikara, T., & Bishop, P. O. (1968). Binocular interaction on single units in cat striate cortex: Simultaneous stimulation by single moving slit with receptive fields in correspondence. *Experimental Brain Research*, *6*, 391–410.

Poggio, G. F., & Poggio, T. (1984). The analysis of stereopsis. *Annual Review of Neuroscience*, *7*, 379–412. https://doi.org/10.1146/annurev.ne.07.030184.002115

Priebe, N. J. (2008). The relationship between subthreshold and suprathreshold ocular dominance in cat primary visual cortex. *The Journal of Neuroscience*, *28*(34), 8553–8559. https://doi.org/10.1523/JNEUROSCI.2182-08.2008

Priebe, N. J., & Ferster, D. (2005). Direction selectivity of excitation and inhibition in simple cells of the cat primary visual cortex. *Neuron*, *45*(1), 133–145. https://doi.org/10.1016/j.neuron.2004.12.024

Priebe, N. J., Mechler, F., Carandini, M., & Ferster, D. (2004). The contribution of spike threshold to the dichotomy of cortical simple and complex cells. *Nature Neuroscience*, *7*(10), 1113–1122. https://doi.org/10.1038/nn1310

Prince, S. J. D., Cumming, B. G., & Parker, A. J. (2002). Range and Mechanism of Encoding of Horizontal Disparity in Macaque V1. *Journal of Neurophysiology*, *87*, 209–221.

Read, J. C. A., & Cumming, B. G. (2003). Testing quantitative models of binocular disparity selectivity in primary visual cortex. *Journal of Neurophysiology*, *90*(5), 2795–2817. https://doi.org/10.1152/jn.01110.2002

Roe, A. W., Parker, A. J., Born, R. T., & DeAngelis, G. C. (2007). Disparity channels in early vision. *Journal of Neuroscience*, *27*(44), 11820–11831.

https://doi.org/10.1523/JNEUROSCI.4164-07.2007
Scholl, B., Latimer, K. W., & Priebe, N. J. (2012). A retinal source of spatial contrast gain control. *Journal of Neuroscience*, *32*(29), 9824–9830. https://doi.org/10.1523/JNEUROSCI.0207-12.2012
Sclar, G, Maunsell, J. H. R., & Lennie, P. (1990). Coding of image contrast in central visual pathways of the macaque monkey. *Vision Research*, *30*(1), 1–10.
Sclar, G, Lennie, P., & Depriest, D. D. (1989). Contrast Adaptaton in Striate Cortex of Macaque. *Vision Res.*, *29*(7), 147–155.
Sengpiel, F., Baddeley, R. J., Freeman, T. C. B., Harrad, R., & Blakemore, C. (1998). Different mechanisms underlie three inhibitory phenomena in cat area 17. *Vision Research*, *38*(14), 2067–2080. https://doi.org/10.1016/S0042-6989(97)00413-6
Sengpiel, F., Blakemore, C., & Harrad, R. (1995). Interocular suppression in the primary visual cortex: a possible neural basis of binocular rivalry. *Vision Research*, *35*(2), 179–195. https://doi.org/10.1016/0042-6989(94)00125-6
Smith, E. L., Chino, Y. M., Ni, J., & Cheng, H. (1997). Binocular combination of contrast signals by striate cortical neurons in the monkey. *Journal of Neurophysiology*, *78*(1), 366–382.
Smith, E. L., Chino, Y. M., Ni, J., Ridder, W. H., & Crawford, M. L. (1997). Binocular spatial phase tuning characteristics of neurons in the macaque striate cortex. *Journal of Neurophysiology*, *78*(1), 351–365.
Solomon, S. G., & Kohn, A. (2014). Moving sensory adaptation beyond suppressive effects in single neurons. *Current Biology*, *24*(20), R1012–R1022. https://doi.org/10.1016/j.cub.2014.09.001
Truchard, A. M., Ohzawa, I., & Freeman, R. D. (2000). Contrast gain control in the visual cortex: monocular versus binocular mechanisms. *Journal of Neuroscience*, *20*(8), 3017–3032. https://doi.org/20024078
Vilidaitė, G., & Baker, D. H. (2015). Unbiased measures of interocular transfer of motion adaptation. *Perception*, *44*(5), 541–555. https://doi.org/10.1068/p7819
Wagenmakers, E.-J., & Farrell, S. (2004). AIC model selection using Akaike weights. *Psychonomic Bulletin & Review*, *11*(1), 192–196.
Westrick, Z. M., Heeger, D. J., & Landy, M. S. (2016). Pattern adaptation and normalization reweighting. *Journal of Neuroscience*, *36*(38), 9805–9816. https://doi.org/10.1523/JNEUROSCI.1067-16.2016
Wilson, H. R. (2017). Binocular contrast, stereopsis, and rivalry: Toward a dynamical synthesis. *Vision Research*, *140*, 89–95. https://doi.org/10.1016/j.visres.2017.07.016
Zhang, B., Bi, H., Sakai, E., Maruko, I., Zheng, J., Smith, E. L., & Chino, Y. M. (2005). Rapid plasticity of binocular connections in developing monkey visual cortex (V1). *Proceedings of the National Academy of Sciences*, *102*(25), 9026–9031. https://doi.org/10.1073/pnas.0500280102

§§§§§§§§§§§§§§§§§§§§§§

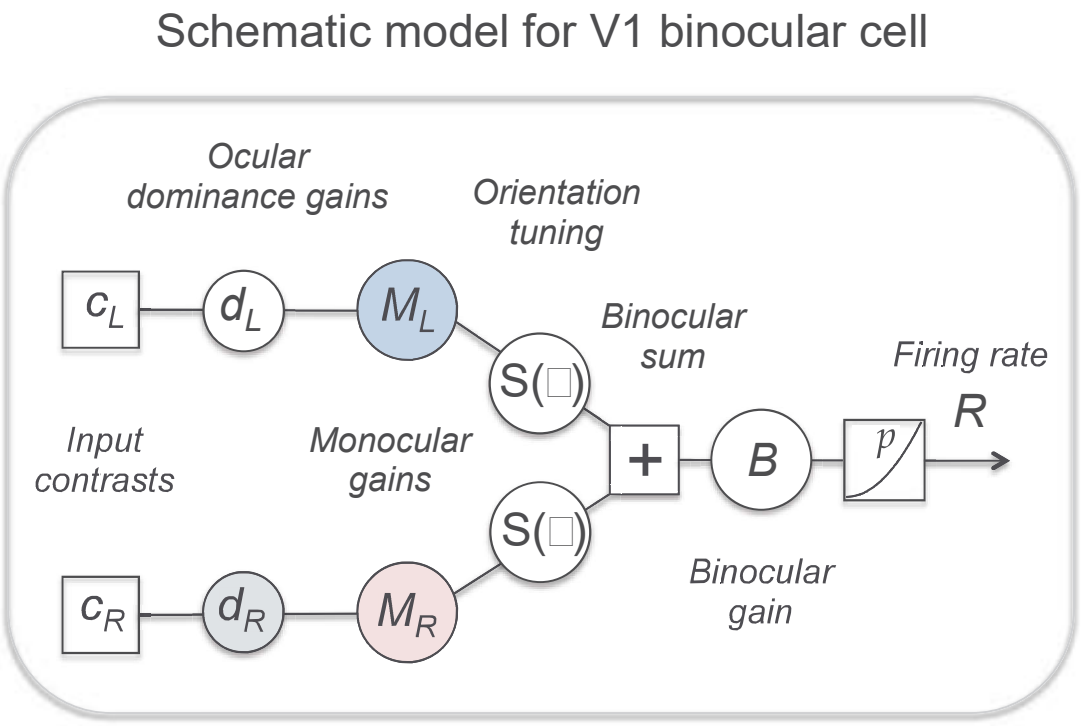

$$R = R_{max}.\{(c_L d_L M_L + c_R d_R M_R).S(\square).B\}^p$$

Figure 1. Schematic model of functional architecture for a binocular cell in V1 (elaborated from Fig. 1B of Truchard *et al*, 2000). We aim here to account for the responses of cat cortical cells to sinewave gratings shown to one eye, with or without prior adaptation to a grating in the same eye or the opposite eye. Monocular and binocular gains (M,B) vary with exposure to the current contrast and any prior (adapting) contrast, while the orientation/direction tuning curve S and ocular dominance gain factors d_L, d_R are taken to be fixed ($0 \leq d_R \leq d_L$). The ratio $d = d_R/d_L$ varies with the degree of ocular dominance (OD) exhibited by the cell. A purely monocular cell would have d=0; a perfectly balanced binocular cell would have d=1. Output values are raised to power p in the conversion to firing rate R.

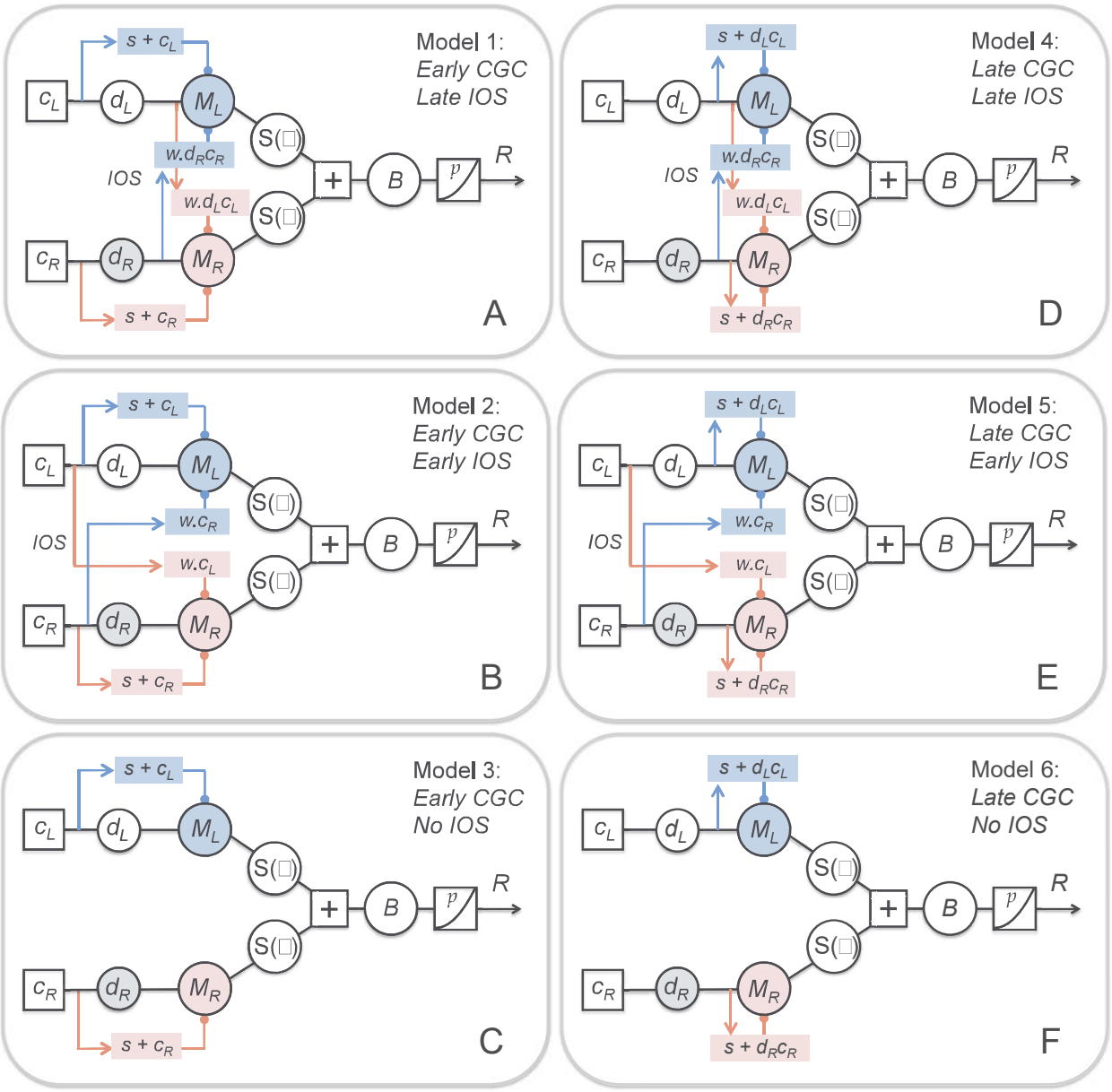

Figure 2. Six variants of the same basic model (Fig. 1). They differ in how the monocular gain mechanisms (M_L, M_R) are organized. Pink or blue lines terminating in filled circles are suppressive (divisive) influences. **A,B,C**: Divisive control of gains M_L,M_R by ipsiocular contrast (c_L,c_R) is 'early', i.e. driven by contrast before any attenuation due to ocular dominance factors (d_L,d_R). **D,E,F**: monocular contrast gain control (CGC) is 'late', arising after OD and driven by the product of contrast and OD factors, ($d_L.c_L$, or $d_R.c_R$). Monocular gain might also be affected by current or prior contrast in the other eye (*interocular suppression,* IOS), and this could arise 'late' (A,D), 'early' (B,E), or not at all (C,F). Strength of IOS was controlled by a weight parameter w. With no IOS, $w = 0$. Responses of all six variants conformed to the same equation (Fig. 1); they differed only in how the M gains depended on contrast, OD and ocularity as sketched here.

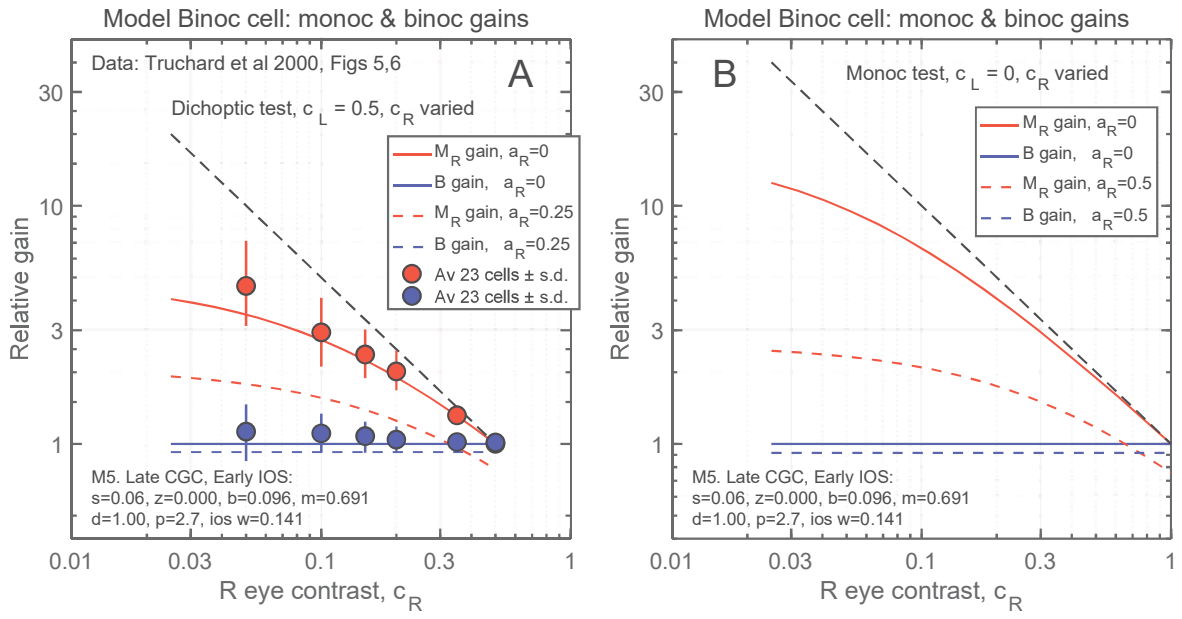

Figure 3. Contrast gain data used to constrain model parameters *s, z*. **A:** Symbols show monocular gains (*M*, red) and binocular gains (*B*, blue) derived from cat V1 cell responses by Truchard *et al* (2000) at each level of R eye contrast when L eye contrast was fixed at 0.5. Highly significant increase of monocular contrast gain (red), but not binocular gain (blue), occurred with decreasing test contrast in one eye. Gains expressed relative to the gain at 0.5 contrast; mean ± s.d. over 23 cells. Solid curves are model gain values for one example model (M5) from eqns. 7.5, 8.5, with s=0.06 chosen to fit the observed *M* gains, z=0 for the *B* gains and with ocular balance (d=1). Agreement between model gains and cat gains was good. All four models with IOS (M1,2,4,5) gave gains similar to those shown, while in the absence of IOS (M3, M6) monocular gains were a bit higher (not shown). Increasing IOS or increasing ocular imbalance (d<1) led to lower monocular gains (not shown). **B:** Model gain values for monocular (R eye) testing, rather than dichoptic. Gains expressed relative to the gain at 1.0 test contrast, as used in the Howarth *et al* (2009) experiments. **A,B:** Dashed lines show predicted impact on gain values of prior adaptation to contrast (a_R). Note that model monocular gains were strongly influenced by test contrast and prior adaptation to contrast, while binocular gains were only slightly altered, if at all.

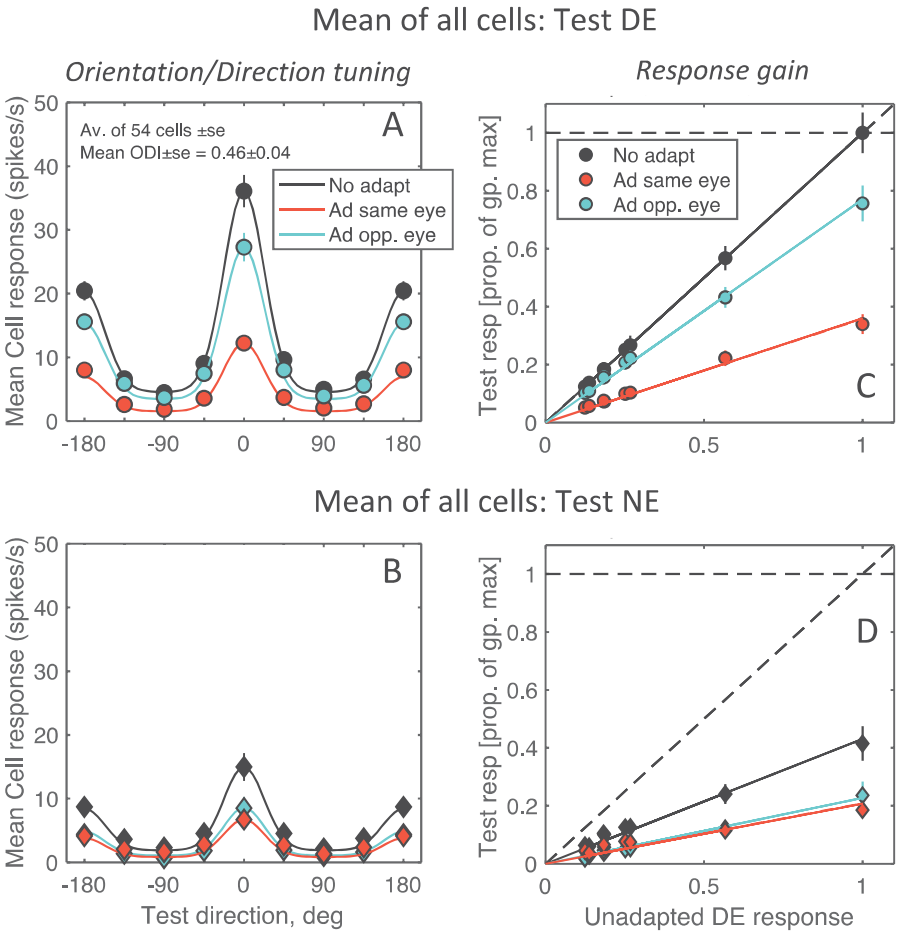

Figure 4. Data overview: mean responses across all 54 cells, when testing the DE (top row) and the NE (lower row). Colours represent unadapted control condition (black); adapting the same eye as the tested eye (red); adapting the opposite eye (cyan). **A,B**: Mean cell responses as a function of test orientation/direction. To describe these data we fitted a curve (see Appendix, Eqn. 14) to the unadapted DE responses (black circles in A), then used this as a template to fit the other 5 conditions simply by scaling the template amplitude to match the peak response in each case. The template shape fitted these mean data strikingly well for both DE and NE, in all three adapting conditions. This implies that, on average, both adaptation and ocular dominance scaled responses down by a common factor across all test orientation/directions. We refer to this scaling factor as the *response gain, G*, and computed it as follows. **C,D**: Data re-plotted from A,B show group mean spike rates normalized to a max. of 1 (i.e. dividing all data by the peak unadapted firing rate seen in panel A). Lines are best-fitting regression lines passing through the origin. Different data points along each line arise from the 8 different test directions (the highest being θ=0, next highest θ=180, and so on). Slopes of these lines are our best estimate of population response gain for a given condition, expressed relative to the unadapted DE gain (panel C, black line).

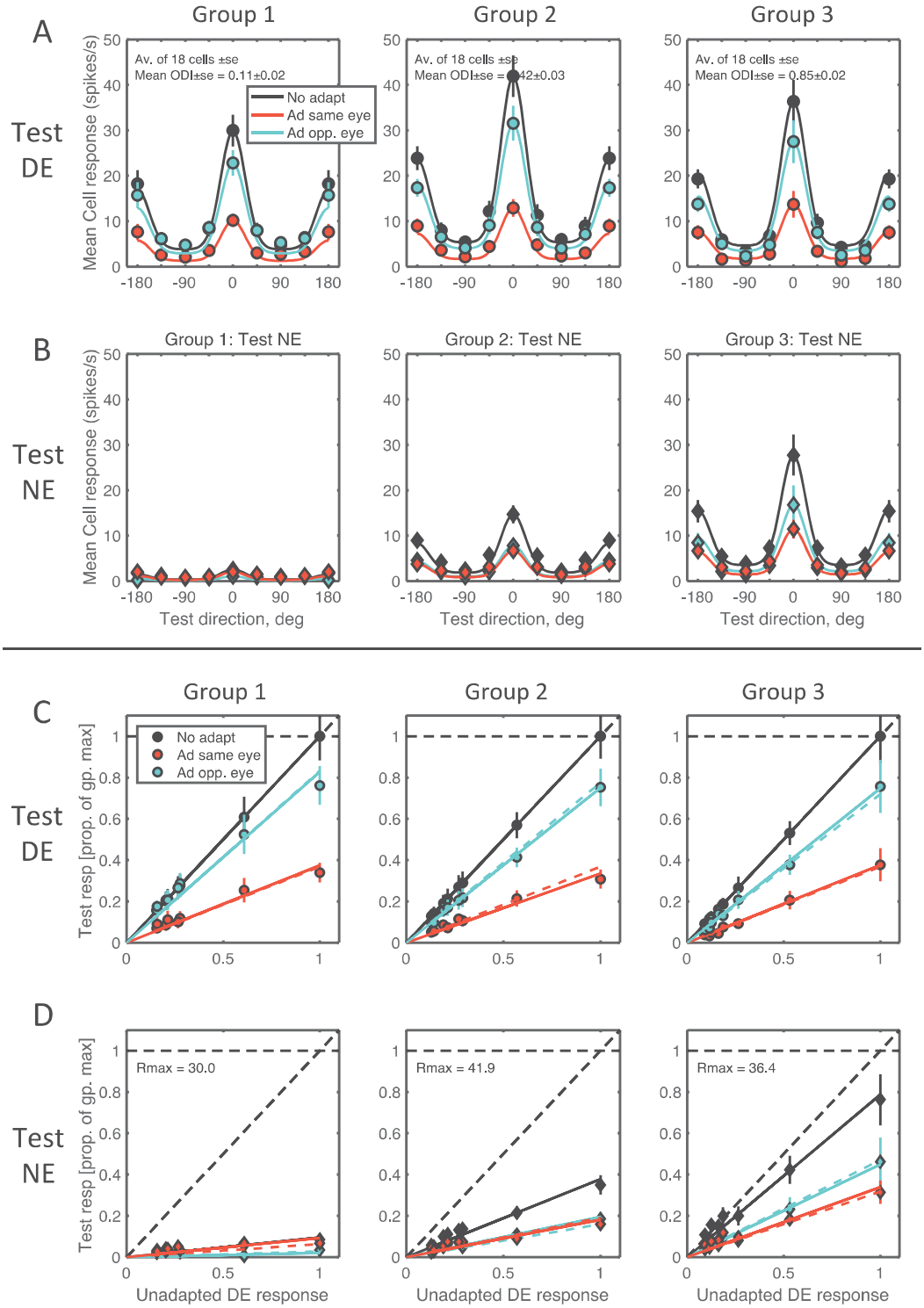

Figure 5. Response tuning curves and derivation of response gains for three cell groups that divided the population according to ODI. Group 1 contains the most ocularly unbalanced cells (mean ODI ± s.e. = 0.11±0.02; *n*=18); group 3 is the most balanced (mean ODI ± s.e. = 0.85±0.02; *n*=18). **A,B**: Mean responses to test grating as a function of test orientation/direction, for the three OD groupings. **A**: test DE; **B**: test NE. Curves show that the same descriptive template (Fig. A1, blue) was a fairly close fit to all the tuning curves for each OD group. Black: no adaptation; red: adapting the tested eye; cyan: adapting the other eye. **C,D**: Response gains for the three OD groups. Data from A,B re-plotted in the same format as Fig. 4C,D. Symbols: group-average cell responses. Solid lines: best-fitting linear regression passing through the origin. The control (unadapted DE) condition has a gain (slope) of 1 by definition (black, row C) and all other conditions had gains < 1. Observed response gains *G* defined in this way can be compared with gains predicted by the fitted model(s) (e.g. dashed lines: model 5).

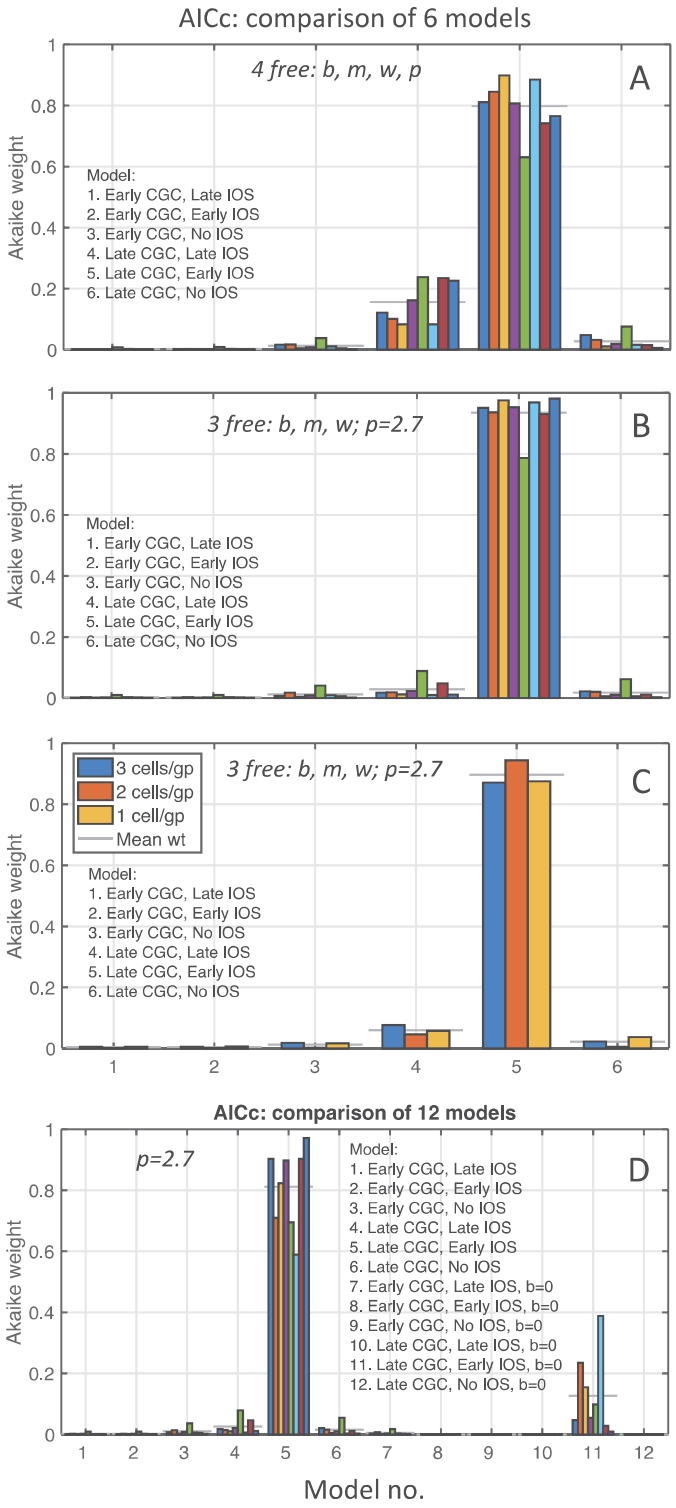

Figure 6. Relative strength of evidence favouring each model (Fig. 2) is compared using the Akaike Information Criterion (AIC), with a standard correction for small sample sizes (AICc). The model with the highest Akaike weight can be interpreted as most likely to be the 'best' model, given the present data (Burnham & Anderson, 2002). Of those models considered in the AIC analysis, the best model is the one closest in information-theoretic terms to an (unknown) true model. **A, B**: Barchart colours represent the number *N* of OD groups into which the cells were divided, ranging from 3 to 10 (left to right respectively). Horizontal grey bars represent mean Akaike weights over these 8 groupings. **A**: with 4 free parameters, the Akaike weights favoured model 5 (late CGC, early IOS), but also lent some support to model 4 (late CGC, late IOS). **B**: When we used two other studies to constrain the output exponent *p* to a fixed value (*p* = 2.7; Fig. 7), then model 5 was uniquely favoured (mean weight = 0.935) while support for model 4 evaporated (mean weight = 0.029). **C**: Model 5 remained the strongly favoured model even with little or no averaging across cells (ie. with 54, 27 or 18 groups, hence 1, 2 or 3 cells per group). **D**: Comparison of 12 models, comprising models 1-6, and models 7-12 which were the same as 1-6, except binocular adaptation parameter *b*=0. Model 5 remained the strongly favoured model, with slight support for model 11 (ie. model 5 with *b*=0).

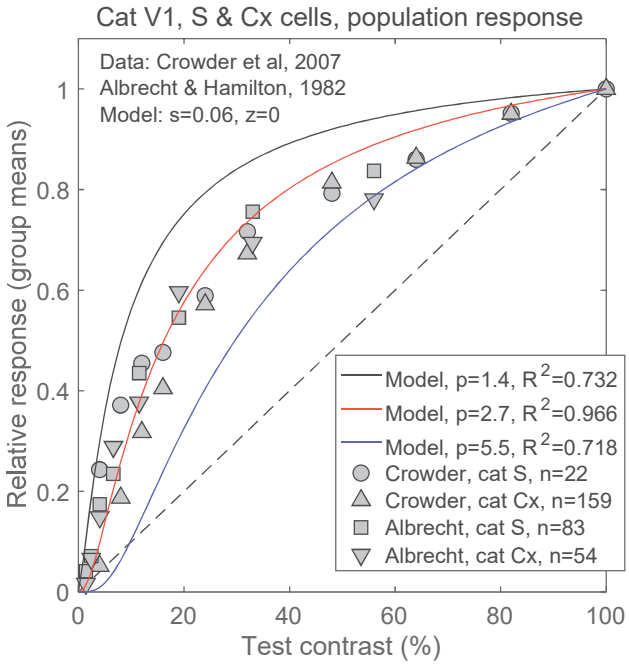

Figure 7. Monocular contrast-responses of cat cortical cell populations. Symbols are mean responses of cat V1 cells, either simple (S) or complex (Cx) from two previous studies; number of neurons in each cell group is shown in legend. Response values were normalized to 1 at 100% contrast. Curves show the DE response of our gain-control model as a function of contrast; all 6 variants were equivalent for this purpose. As expected, the model contrast-response curves varied with output exponent p. Given a fixed value for s (s=0.06) the best-fitting value of p (highest R^2=0.97) was p=2.7 (red curve). Response curves for two sub-optimal values of p are also shown. Fig. 6B showed that constraining all 6 models to have a plausible contrast response (p=2.7) increased the weight of evidence in favour of model 5 and against model 4.

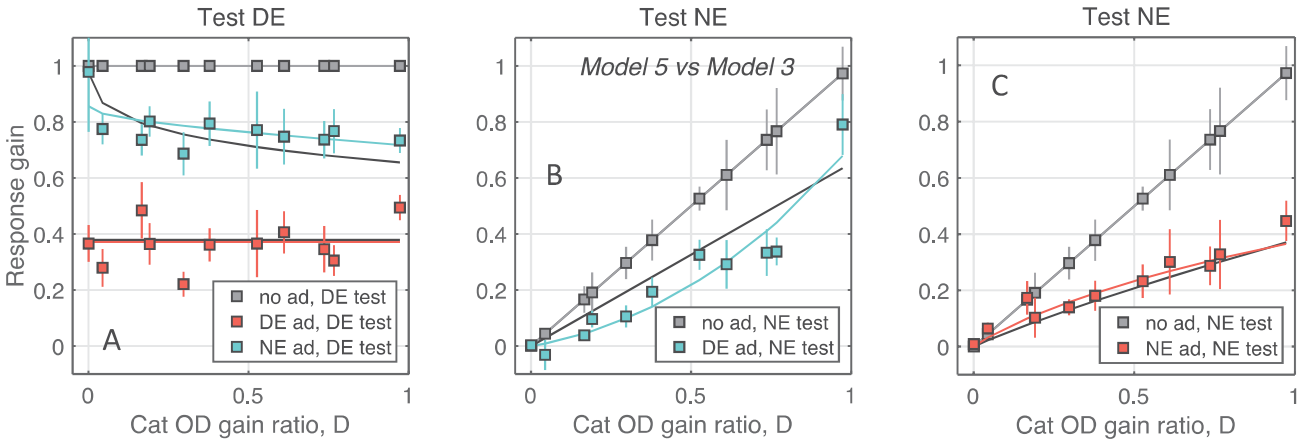

Figure 8. Cat response gains (symbols) and best-fitting model gains (curves) compared for N=11 OD groups, chosen here to cover the full range of D. Each panel compares two models: the best-fitting one (M5, coloured curves) and the simplest one (M3, black curves). [Models 1,2,3 gave essentially identical results]. The x-axis identifies the cell groups by their OD gain ratio (D) – the ratio of unadapted response gains (NE/DE) for each cell group. D = 1 implies perfect ocular balance; lower values imply greater imbalance. There were three adapting conditions: blank adaptation (grey), adapt & test the same eye (red), adapt & test opposite eyes (cyan). Error bars are 95% confidence limits on the cat response gain values. **A:** Test DE, adapt DE or NE; **B:** adapt DE, test NE; **C:** adapt NE, test NE. Same-eye conditions (red) did not distinguish the models, but the interocular conditions (cyan) revealed that M5 fits more closely than M3, and captures better the trends of adapted gain across OD. Parameter values here for M5 were s=0.06, z=0, b= 0.075, m=0.74, p=2.7, w= 0.16, R^2 = 0.95, n data = 44. Only 3 parameters were adjusted to fit this model (*b,m,w;* same for all cell groups and stimulus conditions). See supplementary Fig. S8 for similar comparisons between M5 and M4, or M5 and M6.

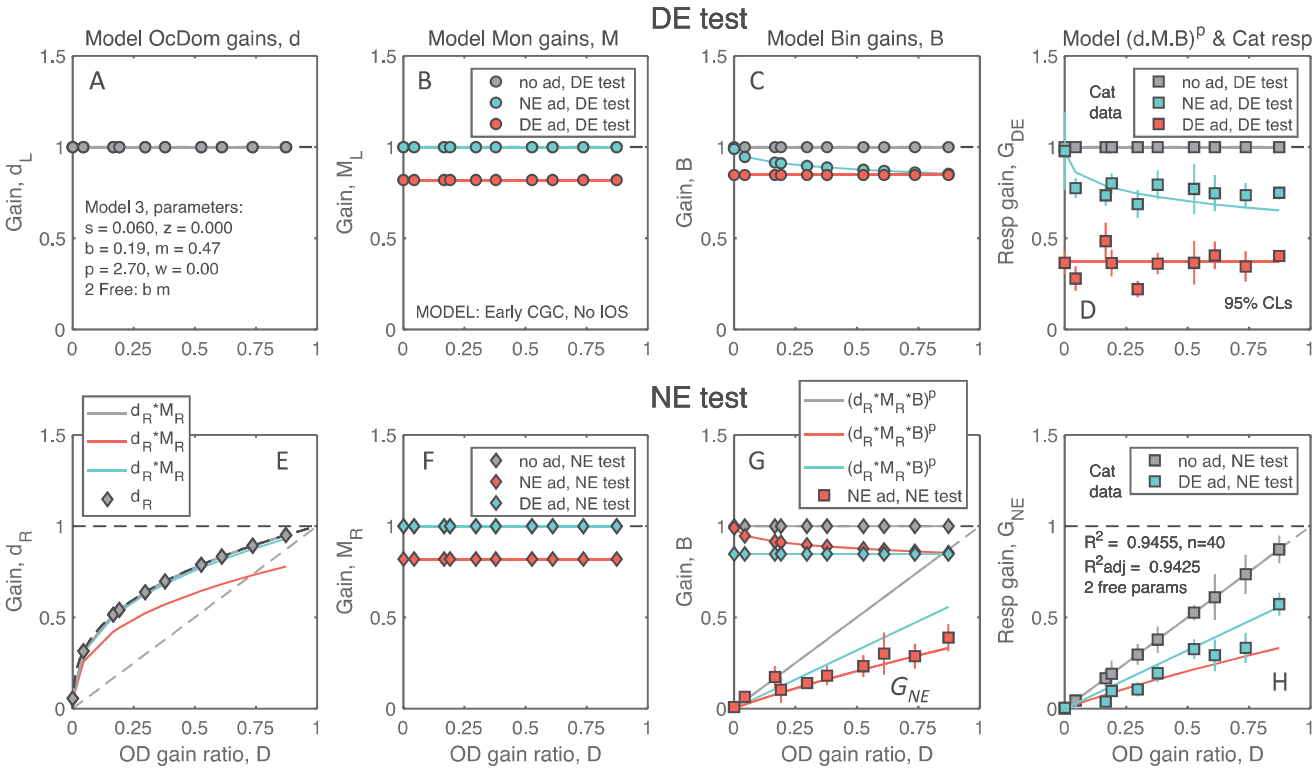

Figure 9. Sources of adaptation and OD in the simplest model, M3: Early CGC, no IOS, applied to N=10 cell groups. **First 3 columns:** attenuation of cell responses after adaptation arises from a sequence of three sources: (i) attenuation (d_R) of the non-dominant input, (ii) reduction of gain (M_L, M_R) at the monocular stage, and (iii) variation of gain (B) at the binocular stage. Subscripts L,R refer to the *tested* eye and for simplicity of presentation we presumed L = *DE*, R = *NE*. Responses in the model were scaled so that the gains d_L, M_L, B had a value of 1 for the DE in the no-adapt condition (top row, grey; hidden behind cyan in B,F). Effects of adaptation and ocular dominance are seen where the d, M, or B terms deviate from 1. **Fourth column:** model response gains are the product of the three gain factors ($d.M.B$, subscripted by L or R as appropriate; eqn. 6) raised to the power p. Solid lines plot this prediction $(d.M.B)^p$, when testing the DE (top row) or NE (lower row), to be compared with the physiological results (filled squares) expressed as cell response gains for each OD group and adapting condition. Error bars are 95% confidence limits on cat response gains. Least-squares model fitting and R^2 goodness-of-fit (inset) were computed only over the adapted conditions. To avoid confusing overlap, cat gain data for DE adapt, NE test (red squares) are plotted in the lower part of panel G (instead of panel H), along with copies of the model curves. Best-fitting parameter values are in panel A.

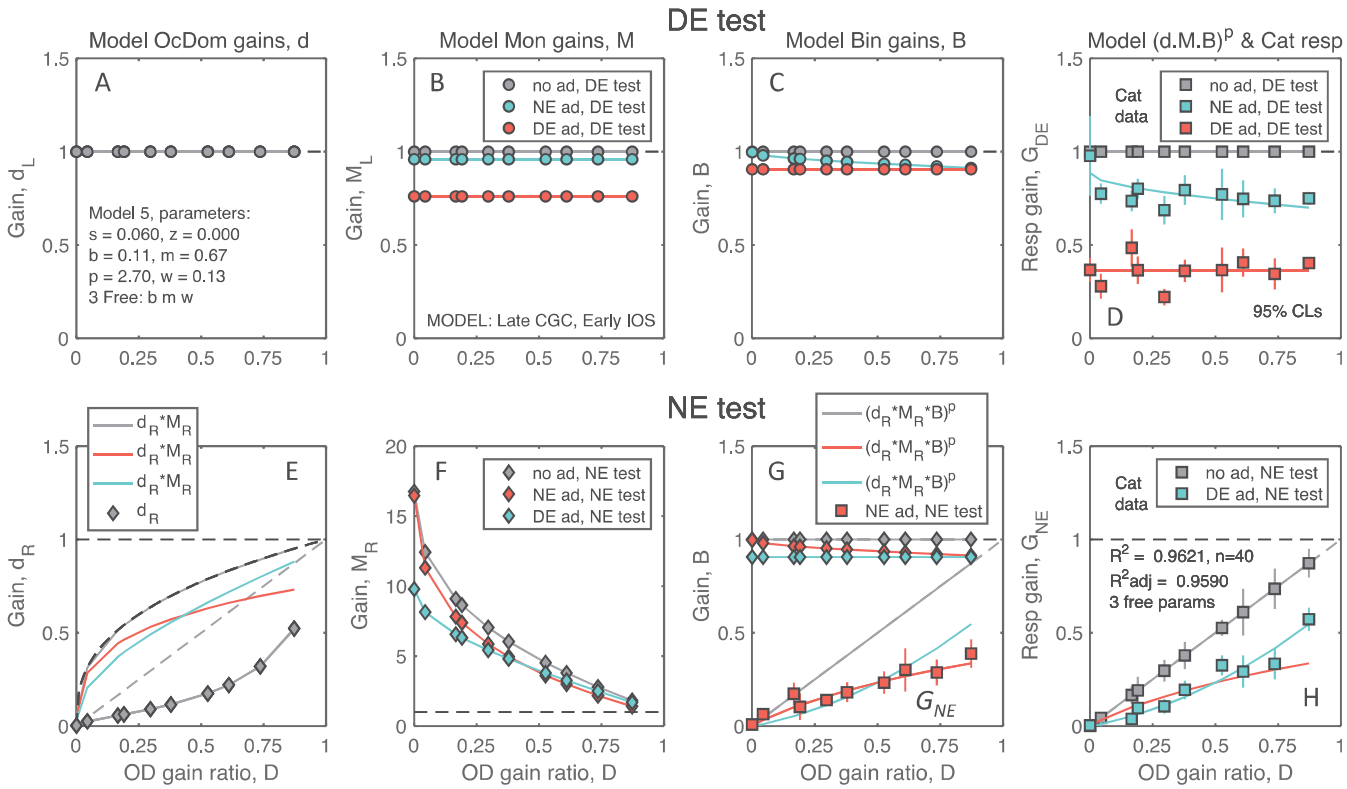

Figure 10. Sources of adaptation and OD in the best-fitting model, M5: Late CGC, Early IOS with N=10 OD groups. Figure layout is the same as Fig. 9. With late CGC, monocular gain M_R increases greatly (panel F) when the suppressive signal is attenuated by OD (at low values of D). This loss of suppression and rise in gain does not occur with early CGC (Fig. 9F), where the divisive suppression is independent of OD. The effective monocular gain for each adapting condition is given by the product $d_R.M_R$ (upper curves in panel E), and this allows easier comparison between early and late CGC models (Fig. 9E *vs* Fig. 10E). Compared with M3, the best-fitting model M5 shows greater adaptation at the monocular level (panel B) and less at the binocular level (panel C).

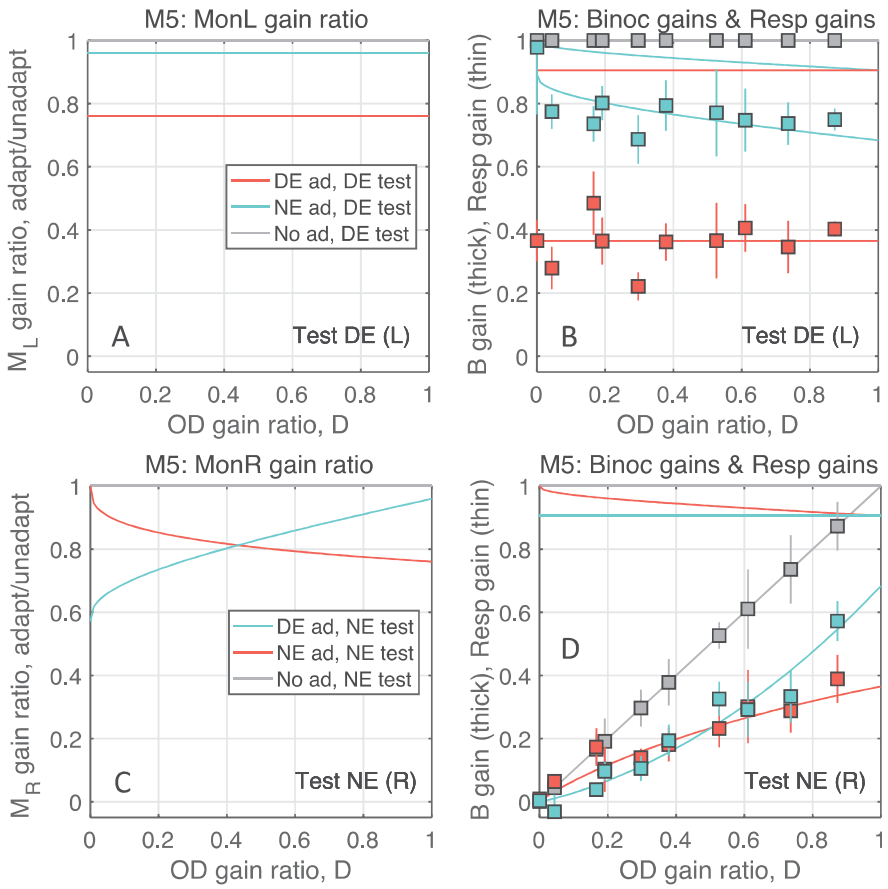

Figure 11. A closer look at the *M* and *B* gain changes for model 5 (late CGC, early IOS), as a function of the OD gain ratio *D*. **A,C:** ratio of adapted model gain to unadapted. Baseline value of 1 means no adaptation effect; lower values imply increasing loss of gain after adaptation. **B,D**: *B* gain (thick curves) or final output response gain (thin curves). Symbols: cat data. Upper legend applies to A, B (test DE); lower legend applies to C, D (test NE). **A**: Gains M_L for the dominant eye (DE) are reduced uniformly after DE adaptation (red line) because DE's input to the CGC is unaffected by OD. After adaptation of the other eye (NE) the model gains M_L are more modestly reduced – by IOS – and these are also uniform (cyan line) because, with *early* IOS, the suppressive signal escapes the substantial attenuation d_R that comes with late IOS. **B**: Gains *B* after DE adaptation are also uniformly reduced (thick red line) for the same reason as in A. The net result is a large, uniform drop in response gain [$(d_L.M_L.B)^p$, thin red line] after DE adaptation. But after NE adaptation, *B* gains fall smoothly with increasing *D* (thick cyan curve) because NE's input to the *B*-gain suppressive mechanism increases with *D*. The result is a much smaller overall loss of gain after NE adaptation (thin cyan curve) that shows a shallow decline with increasing *D*. **C**: Gain changes for the non-dominant eye (test NE) show a *crossover* effect that is characteristic of model M5 (and M4), but not M1,2,3,6. The effect of adaptation on *M* gain either increases with *D*, or decreases, depending on which eye is adapted. **D:** The crossover effect carries through to the final response gain (thin curves), and is seen fairly clearly in the data. See also Fig S7, lower row.

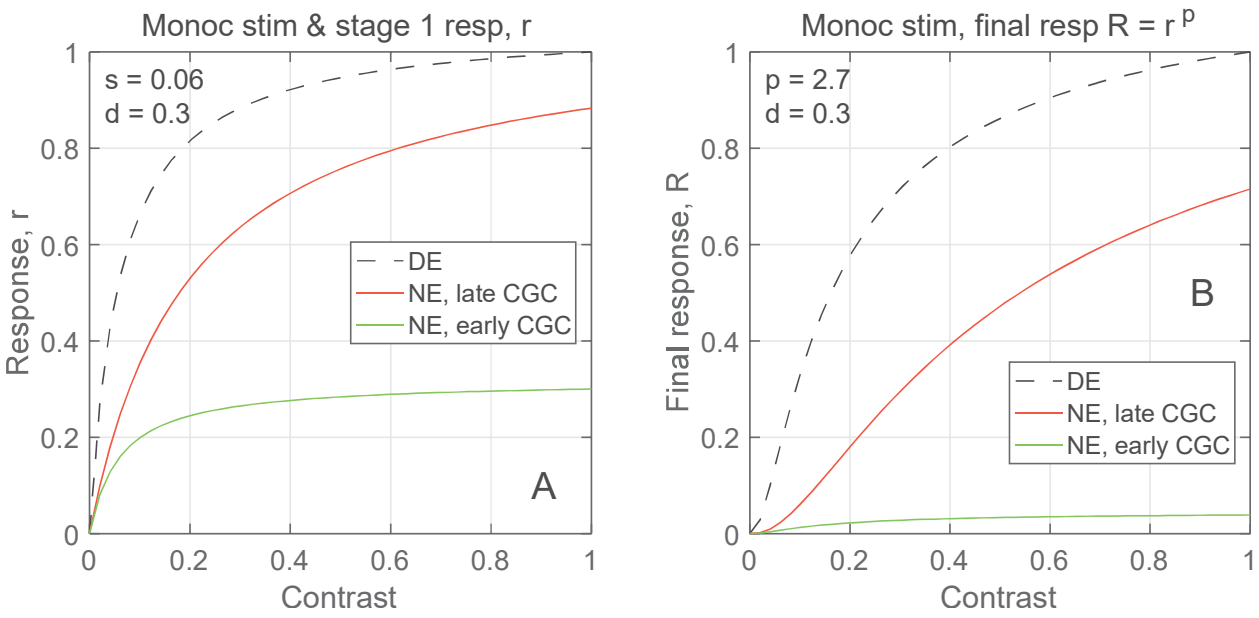

Figure 12. Late CGC (red) compensates for input attenuation by ocular dominance, but early CGC (green) does not. **A:** Model contrast responses *r* at the monocular processing stage, for monocular stimuli to the dominant eye (DE, dashed curve), or the non-dominant eye (NE) with early CGC (green) or late CGC (red). Equations for these curves are: $r_{DE} = k.c/(s+c)$, $r_{NE} = k.d.c/(s+c)$ [early CGC], $r_{NE} = k.d.c/(s+d.c)$ [late CGC], where $k = 1+s$ and c is stimulus contrast. **B:** final 'spike-rate' responses *R* to the same monocular stimuli. Attenuation due to OD (green) is exaggerated by the output nonlinearity (p), but the relative compensation afforded by late CGC (red) is even greater than at the earlier stage (A).

Figure A1 for Appendix

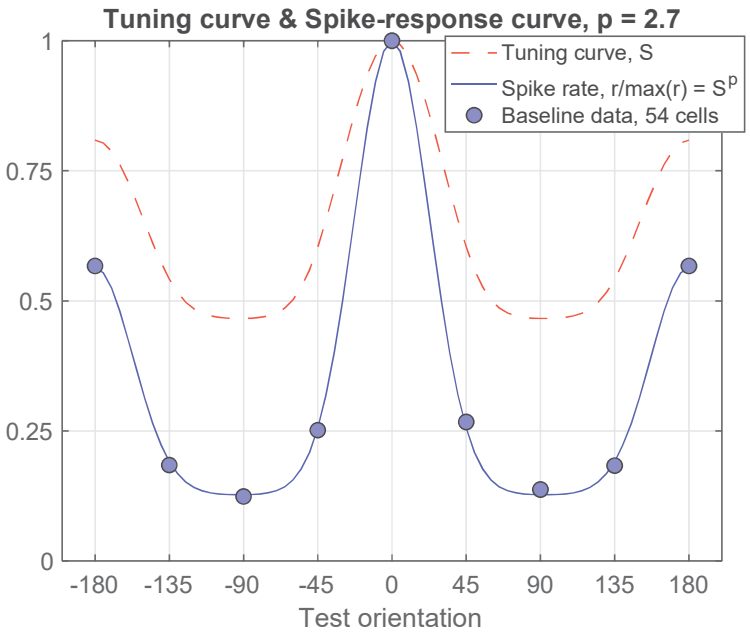

Figure A1. Orientation/direction tuning. Symbols show unadapted baseline spike-rate responses for DE test, averaged over all 54 cells, then normalized to a peak of 1. Solid curve is the (normalized) fitted function $r(\theta)$, eqn. 14. The model's internal tuning curve $S(\theta)$ (dashed curve) was derived from $r(\theta)$, as $S(\theta) = [r(\theta)/max(r)]^{1/p}$.

§§§§§§§§§§§§§§§§§§§§§§

Supplementary Material 1. Graphs

Click here to access/download

Supplementary Material

Georgeson & Sengpiel Supplementary material R1.docx

Credit Authorship Statement

Mark Georgeson: Conceptualization, Methodology, Software, Formal analysis, Writing - Original Draft, Writing - Review & Editing, Visualization, Funding acquisition.

Frank Sengpiel: Conceptualization, Methodology, Investigation, Resources, Writing - Review & Editing, Funding acquisition.